Development of a Novel IoT on Power Structures in Ice Storms Conditions

by

Mohammad Mahdi SHABANI SHAHREZA

THESIS PRESENTED TO ÉCOLE DE
TECHNOLOGIE SUPÉRIEURE IN PARTIAL FULFILLEMENT OF A
MASTER'S DEGREE WITH THESIS IN CONSTRUCTION ENGINEERING
M.A.Sc.

MONTREAL, JANUARY 02, 2025

ÉCOLE DE TECHNOLOGIE SUPÉRIEURE
UNIVERSITÉ DU QUÉBEC

BOARD OF EXAMINERS

THIS THESIS HAS BEEN EVALUATED

BY THE FOLLOWING BOARD OF EXAMINERS

Mr. Michel Kadoch, Thesis Supervisor
Department of Electrical Engineering at École de Technologie supérieure

Mr. René Jr. Landry, President of the Board of Examiners
Department of Electrical Engineering at École de Technologie supérieure

Mr. David Bensoussan, Member of the jury
Department of Electrical Engineering at École de Technologie supérieure

THIS THESIS WAS PRENSENTED AND DEFENDED

IN THE PRESENCE OF A BOARD OF EXAMINERS AND PUBLIC

ON DECEMBER 9, 2024

AT ÉCOLE DE TECHNOLOGIE SUPÉRIEURE

ACKNOWLEDGMENTS

I wish to express my deep gratitude to my dedicated supervisor, Professor Michel Kadoch, for his invaluable guidance, unwavering support, and expert mentorship throughout the development of this thesis. His insightful feedback, patient encouragement, and genuine belief in my abilities have been instrumental in shaping my research and refining my ideas. This thesis stands as a testament to his dedication, and I am honored to have had the privilege of working under his tutelage.

I would also like to extend my heartfelt appreciation to my fiancée, Zeinab, for her unwavering support, patience, and encouragement throughout this journey. Her understanding and belief in me have been a constant source of strength. To my parents, I owe an immense debt of gratitude for their unconditional love, sacrifices, and support. Their guidance and faith in my abilities have been the foundation upon which all my achievements rest. Lastly, I would like to thank my brother, Hadi, for his constant encouragement and for always being there for me. His support and camaraderie have been invaluable throughout this process.

Développement d'une nouvelle technologie IoT pour les infrastructures électriques en conditions de tempêtes de glace

Mohammad Mahdi SHABANI SHAHREZA

RÉSUMÉ

Les événements de pluie verglaçante sont généralement considérés comme la principale cause de défaillance structurelle ou de perte de fonctionnalité d'une large gamme de systèmes structurels dans les régions froides. Par conséquent, la préoccupation principale des études récentes est de rechercher une solution pour prédire soit les risques potentiels (par exemple, l'accumulation de glace et les actions du vent), soit d'estimer le risque induit par la pluie verglaçante. Dans un premier temps, la présente étude développe un cadre d'ingénierie de la pluie verglaçante basé sur la performance (PBFRE) pour l'estimation du risque potentiel lors des événements de pluie verglaçante, en s'appuyant sur la théorie de la probabilité totale. Le cadre PBFRE est principalement décomposé en différents modules, à savoir l'analyse des dangers, la caractérisation structurelle, l'analyse d'interaction, l'analyse structurelle, l'analyse des dommages, l'analyse des pertes, et la prise de décision. Ensuite, il exprime les sources d'incertitudes lors des événements de pluie verglaçante et définit les attentes en matière de performance. De plus, l'application du cadre PBFRE est illustrée à travers une évaluation des risques d'un système de ligne de transmission soumis à des événements de pluie verglaçante. En outre, l'effet de l'utilisation de différents modèles empiriques de prédiction de l'accrétion de glace est mis en évidence. De plus, pour étudier la réponse du système glacé, un modèle par éléments finis, comprenant trois pylônes de transmission et certains conducteurs, est développé. Divers défis empêchent l'application du cadre PBFRE à des échelles structurelles et spatiales. Par exemple, le coût computationnel pour résoudre le problème de risque est intense et augmente considérablement lorsqu'il s'agit d'appliquer le cadre PBFRE à la conception de réseaux étendus dans de vastes régions géographiques. En outre, les effets du changement climatique modifient le taux et l'intensité des précipitations, ce qui modifie finalement les schémas climatologiques, et la plupart des cadres développés jusqu'à présent ne tiennent pas compte de ces changements. Par conséquent, dans le cadre PBFRE, des potentiels sont conçus pour exploiter les capacités des algorithmes avancés d'apprentissage automatique afin de résoudre le coût computationnel requis et de l'Internet des objets (IoT) pour prendre en compte les variations des schémas climatologiques. Les résultats ont révélé que l'utilisation d'un modèle empirique a un impact fondamental sur la conception et la maintenance des systèmes structurels sujets à la pluie verglaçante. De plus, l'intégration des principes de l'IoT entraîne une modification significative de la prédiction de la pluie verglaçante extrême, ce qui pourrait littéralement affecter les coûts des mégaprojets.

Mots-clés : pluie verglaçante, ingénierie basée sur la performance, internet des objets, accumulation de glace, risque, apprentissage automatique

Development of a novel IoT on power structures in ice storms conditions

Mohammad Mahdi SHABANI SHAHREZA

ABSTRACT

Freezing rain events are typically considered as the primary cause of structural failure or loss of functionality of a wide range of structural systems in cold regions. Consequently, the primary concern of the recent studies is to look for a solution to predict either the potential hazards (e.g., ice accumulation and wind actions) or estimate freezing rain-induced risk. In the first step, the current study develops a Performance-Based Freezing Rain Engineering (PBFRE) framework for estimation of the potential risk during freezing rain events based on theory of the total probability. PBFRE framework is mainly decomposed in different modules, namely hazard analysis, structural characterization, interaction analysis, structural analysis, damage analysis, loss analysis, and decision-making. Then, it expresses source of uncertainties during freezing rain events and defines performance expectations. Additionally, the application of the PBFRE framework is then illustrated through risk assessment of a transmission tower-line system prone to freezing rain events. Additionally, the effect of employing different empirical ice accretion prediction model is highlight. Moreover, to investigate the response of the iced system, a Finite Element model consisting of three transmission towers and some conductors are developed. Various challenges prevent the application of PBFRE framework at structural and spatial scales. For instance, the computational cost for solving the risk problem is intense and it increases dramatically when it comes to applying the PBFRE framework for designing extended networks at extensive geographical regions. In addition, climate change effects are changing the precipitation rate and intensity that eventually changes the climatological patterns and most of so far developed framework are not accounted for such changes. Therefore, in the PBFRE framework potentials are designed to leverage the capabilities of advanced machine learning algorithms for solving the required computational cost and Internet of Things (IoT) to account for variation in climatological patterns. The results revealed the importance of employing empirical model has a fundamental impact of design and maintenance of structural systems prone to freezing rain. In addition, integration of IoT principles results in significant change in extreme freezing rain prediction which could literally affects the megaproject costs. In addition, utilizing advanced machine learning algorithms led to immediate prediction and reduce the prediction time by more than 98%.

Keywords: freezing rain, performance-based engineering, internet of things, ice accretion, risk, machine learning

TABLE OF CONTENTS

LIST OF TABLES

Page

LIST OF FIGURES

LIST OF ABREVIATIONS AND ACRONYMS

ACSR	Aluminum conductor steel-reinforced cable
AI	Artificial Intelligence
ANN	Artificial Neural Network
ASOS	Automated Surface/Weather Observing Systems
BCR	Benefit-Cost Ratio
BLUP	Best Linear Unbiased Predictions
CHBDC	Canadian Highway Bridge Design Code
CSA	Canadian Standard Association
CRREL	Cold Regions Research and Engineering Laboratory
DM	Damage Measures
DV	Decision Variables
EDP	Engineering Demand Parameters
EOM	Equation of Motion
ETL	Extract, Transform, and Load
FFNN	Feed Forward Neural Network
FE	Finite Element
FOSM	First-Order Second-Moment
FZ	Freezing
FZDZ	Freezing Drizzle
FR	Freezing Rain
SciPy	Fundamental algorithms for scientific computing in Python
GEV	Generalized Extreme Value distribution

GAN	Generative Adversarial Network
GWO	Grey Wolf Optimizer
IM	Intensity Measures
IP	Interaction Parameters
ISO	International Standard Organization
IoT	Internet of Things
ML	Machine Learning
METAR	Meteorological Aerodrome Report
OK	Ordinary Kriging
PEER	Pacific Earthquake Engineering Research Center
PBE	Performance-Based Engineering
PBFE	Performance-Based Fire Engineering
PBFRE	Performance-Based Freezing Rain
PBHE	Performance-Based Hurricane Engineering
PBIE	Performance-Based Ice Engineering
PBSE	Performance-Based Seismic Engineering
PBTE	Performance-Based Tsunami Engineering
PBWE	Performance-Based Wind Engineering
PIDL	Physics-Infromed Deep Learning
PC	Polynomial Chaos
SINDy	Sparse Identification of Nonlinear Dynamics
SP	Structural Parameters
US	United States

LIST OF SYMBOLS

Latin alphabet

A	The cross section of the cable
$A_{ext,iced}$	Cross-sectional area of the iced surface
C	Load combination
D_{tot}	The accumulated damage
$E_{t,i}$	Measured/estimated environmental parameters at time t
G_C	Combined wind factor
G_L	Span factor
H	Horizontal tension component
H_g	Depth of liquid precipitation
H_{max}	Maximum height
H_{min}	Minimum height
L	Span length
L	The applied load or demand on the structure
M	The total mass of accreted ice within the period of Δt
n	The total number of involved intensity measures in freezing rain events
n_i	The number of cycles during ith experiment

N_i	The number of cycles that could lead to structural failure due to load
P	Precipitation rate
q_0	Dynamic wind pressure
R	The resistance or capacity of the structure
R_{eq}	The uniform radial ice thickness
S_{in}	Structural conditions (intact or aged)
T_0	Predefined fatigue life for the conductor
T_{fat}	Fatigue life of the conductor
T_{min}	Minimum temperature
T_{max}	Maximum temperature
T_h	Total freezing precipitation for one hour interval
u	The structural status / unit function
V_0	Wind speed measured at height z_0
V_d	Mean wind speed
W_t	The liquid water content

Greek alphabet

βL	Particular symmetric vertical modal component
ε_t	Total damping
η	A constant that should be determined for each material
ρ_{air}	Density of air
ρ_w	Density of water
φ_n	Nth symmetric in-place mode shape
χ	Experts comments/decision(s)
ω_n	Natural frequency of nth mode
ξ_a	Aerodynamic damping
ξ_s	Structural damping

INTRODUCTION

0.1 Background and problem statement

Atmospheric icing which is primarily seen in the northern countries like Canada, United Kingdom, Iceland, Finland and Russia can impact the integrity of a wide variety of structural systems, such as transmission systems, wind turbines, and photovoltaic panels (Fikke et al., 2008). In general, atmospheric icing (aka icing conditions) is defined as an ice layer which sticks and accumulates on a surface because of supercooled water droplet impact with the target surface. This ice layer can literally alter the aerodynamic behavior of impinged surface, causing loss of functionality or even structural collapse. In higher altitudes, structural systems are typically prone to rime icing, whereas structures are suffering from wet snow or freezing rain in lower altitudes.

The ice accretion process has been primarily a source of inspiration for conducting research in the aeronautics industry. Four classifications were proposed for facilitating the understanding of icing impact on the aircraft performance, namely trace, light, moderate, and severe. Numerous studies can be found in the literature discussing the nature and source of accretion process (i.e., nucleation). However, civil engineering is historically the one which includes ice accretion research.

The major concern during an icing condition is accumulation of a thick ice layer on wired structures because the ice layer changes the aerodynamic behavior of the impinged surface causing aerodynamic instabilities. In addition, the formed ice layer poses an extra vertical load (i.e., its weight) which produces tension in the cable and transmits it to the supportive towers. For instance, during visual inspection which was carried out in Norway, the ice thickness was measured to be maximum 30 cm (305 $^{kg}/_{m}$)(Makkonen, 2000). Another example could be the North American 1998 that prevailed some parts of Canada and United States, caused

several fatalities and over three billion dollars lost (Lecomte et al., 1998). Unlike other climatological parameters, such as wind speed, ice accumulation is rarely measured during icing conditions in weather. In addition, icing conditions are typically characterized as short, rare, and intense events that makes this gap of data wider.

Alternative approaches are employed for estimation of ice accretion on transmission cables, namely mathematical methods, empirical and experimental observations, probabilistic mapping, and de-icing approaches(Pohlman & Landers, 1982). Numerous studies can be found the literature that have focused on the first group, such as Makkonen (Jones et al., 2004; Makkonen, 1984, 1998, 2000). The outcomes of these studies are generally utilized for structural design and assessment. The other groups may not potentially be suitable for design and assessment of structural systems. These models are basically developed based on the assumption of cylindrical ice shape and ignore the formation phase of the ice layer. However, the combined effect of wind and ice deposit produces vibrations in conductors and may impair their reliability and integrity. Specifically, Wind-induced vibrations occur when asymmetrical ice accretion on wires creates aerodynamic lift, increasing tension on tower supports. Such vibrations can critically damage the system, ranging from conductor strand burn to potential cascade failures(Guerard et al., 2011; McComber, 1984).Codes and standards usually provide overly conservative considerations to cover the adverse effects of wind on iced conductors.

0.2 Objectives

The primary aim of this research is to investigate how the real-time risk of freezing rain events can be estimated accurately and efficiently. To achieve this goal, the current study will investigate different parts in freezing rain-induced risk prediction. For instance, it will highlight which empirical ice prediction model can be more practical in estimation of ice accretion during icing condition. This will reduce the errors originated from overestimation of maximum ice accretion during service time of the system. To achieve that objective, the current study will retrieve and preprocess data from a wide range of weather stations in the United

States, then compare the estimations in terms of different metrics to highlight the differences, especially the recommended model by Canadian Standard Association (CSA) 22.3(CSA Group, 2020) and Cold Regions Research and Engineering Laboratory (CRREL)(Jones, 1996a). Following that, the study will look for high-level and advanced solutions based on Performance-Based Engineering (PBE), Internet of Things (IoT), and advanced data-driven algorithms (e.g., Machine Learning [ML]) to address aforementioned concern. Therefore, the efforts of this study are specifically dedicated to development of a novel framework for prediction of real-time freezing rain-induced risk on structural systems in cold regions.

0.3 Methodology

To achieve the aforementioned goal, following methodology has been developed:

1. Developing a Performance-Based Freezing Rain (PBFRE) framework based on the total probability theorem.
2. Investigating the effect of employing different empirical ice accretion prediction models in estimation of maximum annual ice accretion.
3. Leveraging the capacities of advanced ML algorithms and IoT principles for overcoming the issues related in real-time prediction of freezing rain potential threat(s) to structural systems at different scales, namely structural and spatial.
4. Illustrating the application of the PBFRE framework for risk assessment of a transmission tower-line system in the United States.

0.4 Limitation of the study

The current study has the following restrictions:

1. The interaction between wind actions and ice accumulation should be modeled using icing wind tunnel tests or advanced numerical models based on actual ice shape to make the results more robust; however, the current study is developed based on a simplified model (Poots & Skelton, 1995).

2. The interaction between hazards during an event should be modeled with full details to obtain a clear picture of the risks, even though, the hazards (i.e., ice accretion and wind actions) are considered based on simple procedure (Jones et al., n.d.).
3. The damage analysis and structural analysis modules are considered to be the same for the sake of simplicity of modeling.
4. The loss analysis module is excluded from the study due to the lack of proper financial data and models.

0.5 Thesis organization

The current dissertation comprises four main chapters:

- Chapter 1: An all-inclusive literature review on freezing rain, its adverse effects and predictions models;
- Chapter 2: Employed methodology to develop real-time freezing rain maps;
- Chapter 3: A Novel Performance-Based Framework for Freezing Rain Events (*Journal paper- submitted to the Structural Safety journal*).

CHAPTER 1

LITERATURE REVIEW

1.1 Introduction

This chapter delves into the potential threats of atmospheric icing and complexity associated with prediction of freezing rain events to structural systems. It then discusses different models for prediction of ice accretion during freezing rain. Subsequently, the study explores and explains the interaction of different hazards throughout an icing event. Then, it provides a comprehensive review on PBE principles, its development in different fields, and covers up each module briefly. Finaly, the study highlights the gaps and draws conclusion based on the collected literature review.

1.2 Freezing rain

Freezing rain forms under specific atmospheric conditions characterized by the presence of a warm air layer between two colder layers. The process begins with precipitation originating as snow in the uppermost cold layer, where temperatures are below freezing. As the snowflakes descend, they pass through a warmer layer of air, where temperatures rise above 0°C, causing the snow to melt and turn into rain. This liquid rain continues its descent until it reaches a shallow layer of subfreezing air near the Earth's surface. Unlike sleet, which refreezes before hitting the ground, the rain in freezing rain remains in liquid form as it falls through this shallow cold layer. Upon contact with surfaces that are at or below freezing, the supercooled droplets instantly freeze, forming a layer of ice. This phenomenon is particularly hazardous because it can lead to the rapid accumulation of ice on roads, power lines, trees, and other structures, causing disruptions and dangers such as power outages, fallen branches, and extremely slippery surfaces. The formation of freezing rain requires a precise balance of temperature layers in the atmosphere, making it a relatively rare but impactful weather event(Zerr, 1997).

The formation of freezing rain is influenced by several key environmental factors, with temperature profiles in the atmosphere being the most critical. One of the primary factors is the presence of a warm air layer sandwiched between two colder layers, typically found in a temperature inversion scenario(Kämäräinen et al., 2018). The thickness and altitude of this warm layer determine whether snow will melt into rain as it falls. If the warm layer is sufficiently deep and extends above 0°C, the snowflakes will completely melt into liquid rain before reaching the surface. Another crucial factor is the temperature of the shallow cold layer near the Earth's surface. This layer must be below freezing (0°C) but not thick enough to allow the liquid rain to refreeze into sleet. The surface temperature is also vital, as it needs to be at or below freezing for the supercooled raindrops to freeze upon contact, leading to ice accumulation. Additional environmental factors include the presence of moisture-laden air masses, which provide the necessary precipitation, and the dynamics of the frontal systems that create the necessary temperature inversion. The movement and interaction of warm and cold fronts play a significant role in setting up the temperature profile required for freezing rain. Wind patterns can also influence the distribution and intensity of freezing rain events by affecting the transport of warm and cold air masses.

Freezing rain events basically last hours while their impacts prolong for days and weeks. For instance, North American 1998 ice storm left more than five million houses without electricity for more than a week (Lecomte et al., 1998). According to the study conducted by Hydro-Quebec (McClure et al., 2002), the combination effect of wind actions and ice accretion contributed to collapse of more than 600 transmission towers in Quebec, and breaking of more than 2,500 wooden towers or structural elements of the electrical grid that led to more than two million dollars lost(Fikke et al., 2008). Consequently, ice accumulation on cables poses significant mechanical threats, primarily due to the increased weight and altered structural dynamics. The added mass from ice accretion raises the tensile forces within the cables, leading to higher stress on support structures such as towers and poles. This can result in sagging, increased risk of cable snapping, or even tower collapse under extreme conditions. Additionally, uneven ice buildup can create asymmetrical loads, causing torsional forces and

vibrations that further compromise the cable's mechanical stability. Over time, these stresses can lead to material fatigue, accelerated wear, and potential failure of the system (Snaiki & Shabani, 2023). In addition, Ice accumulation on cables significantly alters their aerodynamic behavior by changing the shape and surface roughness of the cables. The irregular, often asymmetric ice formations can increase aerodynamic drag and lift forces, leading to unpredictable wind-induced vibrations and oscillations. These altered aerodynamic properties can exacerbate mechanical stresses and contribute to the instability of the cables, increasing the risk of structural damage or failure(Waris et al., 2008). Therefore, it is of great importance to evaluate these impacts before the occurrence of freezing rain events.

1.3 Aerodynamic of iced conductors

Transmission tower-line systems are essentially more vulnerable to wind actions due to wind-induced vibrations. Specifically, the wind-induced vibrations in iced conductors can be classified into two main groups, namely aeolian vibrations and wake-induced oscillations(Van Dyke et al., 2008a). If damping systems or spacers cannot attenuate these vibrations, they might impair the reliability and integrity of transmission grid. It should be noted that the amplitude and frequency of aeolian vibrations in presence of an ice layer is fundamentally different from the situation in which the bare conductor is subjected to wind. Therefore, it is of great importance to study and understand the physics of onset and propagation of instabilities in iced conductors. Codes, Standards and design practice typically provide overly conservative considerations to avoid the complexity of conducting dynamic analysis on iced conductors. For instance, CSA C22.3(CSA Group, 2020) recommends choosing maximum of these load combinations for design of transmission lines subjected to freezing rain:

- The 50-years return period of ice accretion in the cylindrical shape with low probability and average of annual maximum 3-seconds gust wind speed.
- The 50-years return period of 3-secods gust wind speed with low probability and average of annual maximum ice accretion in cylindrical shape.

The concerning point about aforementioned recommendation is that it does not necessarily guarantee the integrity and reliability of the system during its service time. In addition, this recommendation can lead to overestimation and overdesigning, consequently (Arriaga, 2020). Therefore, it is crucial to understand when and how wind-induced instabilities onset and propagate in cables.

Among all wind-induced vibrations, galloping could be one that requires the most attention during design and maintenance steps. Basically, galloping is defined as low amplitude and low frequency oscillations in conductors(Jianwei Wang & Lilien, 1998). Galloping begins when the aerodynamic forces acting on a structure, such as a transmission line or a bridge cable, induce self-excited oscillations. These oscillations occur due to a phenomenon where the wind force, instead of stabilizing the structure, reinforces the motion, leading to large, potentially destructive vibrations(Van Dyke & Laneville, 2008). Historically, Den Hartog(Hartog, 1932) was the first who formulated these oscillations. Den Hartog coefficient was defined as the ratio of lift coefficient to the drag coefficient for an iced conductor. Therefore, once the Den Hartog coefficient is negative, galloping can initiate. Later, Scruton stated that negative Den Hartog does not necessarily lead to onset of instabilities and free stream wind speed must be larger than the critical wind speed (SCRUTON & FLINT, 1964). This critical wind speed depends on the shape and orientation of the structure, as well as its stiffness and damping properties. Beyond this speed, the aerodynamic forces acting on the structure become unstable and can initiate oscillations. However, it was proven that negative total damping(Borna, 2014) is other necessary condition for onset of galloping vibrations. The third condition refers to the condition where there is no balance between the aerodynamic and structural damping; the structure is not able to mitigate the oscillations and remains in the self-excited oscillatory motions (Rossi et al., 2020).

The primary step to predict the structural response of the system is to calculate the static loads, which are essentially the mass of accreted ice and wind speed. The ice layer basically creates stresses in the cable and transmits them to the adjacent towers. The stress can be obtained by

based on ideal static response (H. M. Irvine & T. K. Caughey, 1974). The challenging point in the equation is the amount of sag that is different or must be measured. The other static load is the wind-induced force in the horizontal direction. CSA C22.3(CSA Group, 2020) has already formulated the corresponding produced tension in cables. The challenging part in estimation of wind force is drag coefficient, which is a function several factors, such as shape of impinged object, wind speed, and angle of attack(Kyburz et al., 2022). Estimation of drag coefficient necessitates conducting advanced numerical simulations (e.g., (Dwaipayan Sharma et al., 2022)) or carry out icing wind tunnel test (e.g., (Rossi et al., 2020)) that is not affordable and practical. Alternatively, data-driven method (e.g., ML algorithms (Snaiki, 2024)) can be employed to overcome the limitations and issues. In addition, it is crucial to assume a shape for ice objects. Some studies can be found in the literature in this regard. For instance, a semi-elliptical shape was proposed for rime ice icing (Poots & Skelton, 1994, 1995) while complicate shape were recommended for wet icing (P. Fu et al., 2006). Figure 1.1 depicts two ice profiles for snow wet (with runoff) and hard rime.

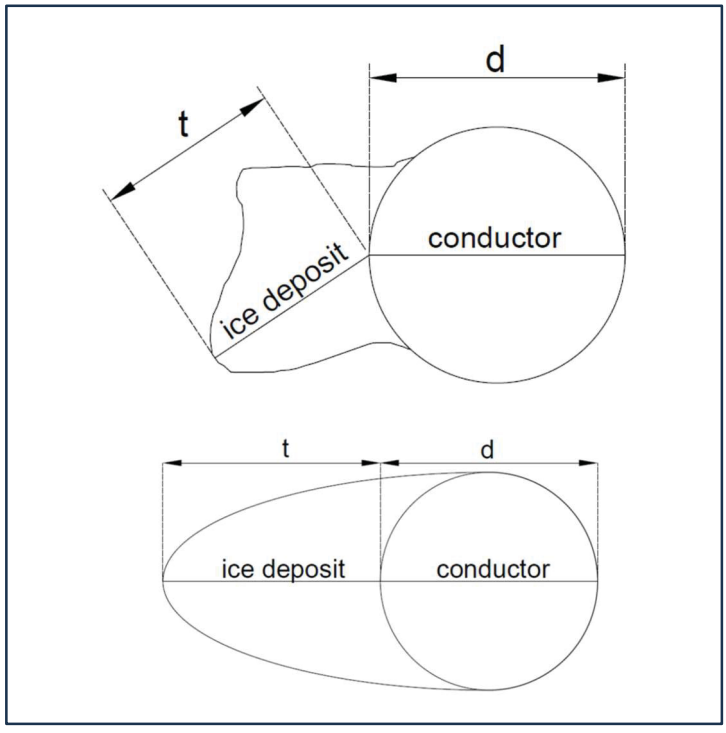

Figure 1.1 Ideal profile for rime ice and wet snow
Taken from (Arriaga, 2020)

To obtain the natural frequency of the iced conductor, the linear theory of suspended cables (H. M. Irvine & T. K. Caughey, 1974) can employed. The theory is limited to conductors with the ratio of sag to span length less than 0.125. The first two modes of oscillations are essentially the most governing and effective modes (Lilien et al., 2005). Determination of those frequencies requires solving an underdetermined equation. For instance, the equation for a 23.55 (mm) conductor subjected to glaze ice is solved using SciPy package in python and is illustrated in following.

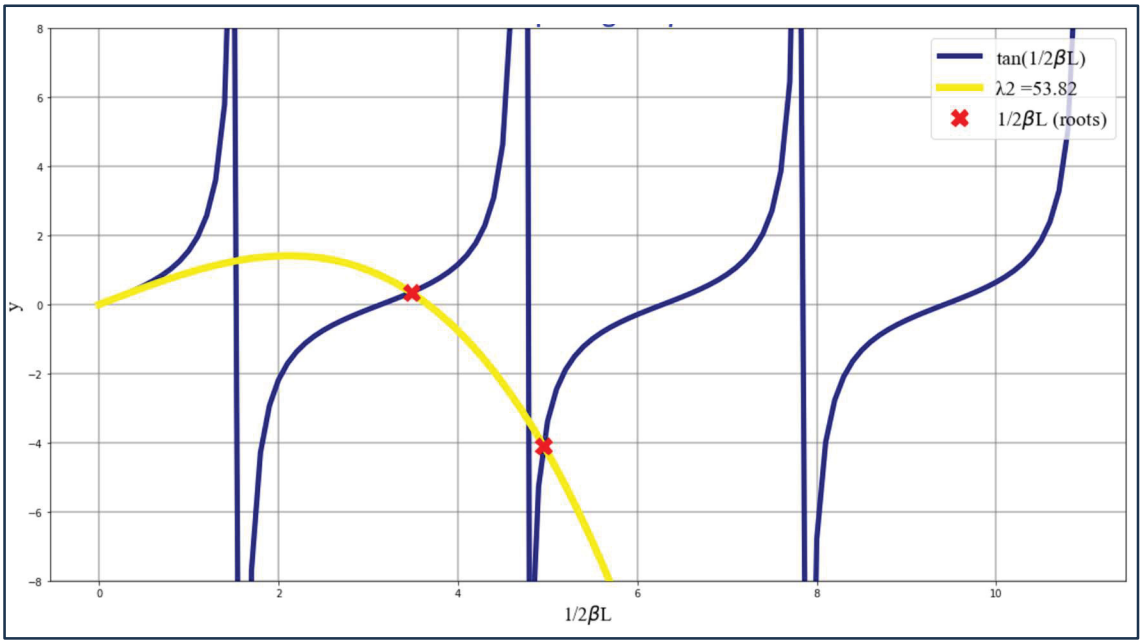

Figure 1.2 Graphical representation of non-zero roots in mode shapes equation for a 23.55 (mm) single conductor

In some studies, determination of the frequencies and the first two mode shapes are done visually or through simplified graphical representation of solutions Figure 1.2. Herein, the symmetric in-plane mode of oscillation is considered and the equation of motion is solved based on the proposed formula by (Arriaga, 2020). The particular symmetric mode shape ($^1/_2\,\beta L$) in the proposed formula was obtained through a numerical approach and it was used

for describing the oscillations of the iced conductor. It should be noted that *y* in the Figure 1.2 indicates the amplitude of vertical oscillations.

However, this approach might not be efficient when ice comes to probabilistic analyses since the structural response must be determined for hundreds or thousands of conditions. The dynamic load, produced by galloping oscillations, is the other load that should be determined before design. The extra load originated by the vertical galloping movements can be obtained through conducting modal analysis and estimation of total displacement of the cable to (Rossi et al., 2020).

1.4 Ice prediction

The life cycle of an ice layer has three steps, namely nucleation and accumulation, persistent, and shedding. Ice nucleation on a surface occurs when water molecules begin to arrange into a crystalline structure, forming the first seeds of an ice layer. This process typically starts at specific sites on the surface, known as nucleation sites, which can be influenced by surface roughness, chemical composition, and temperature(Wang et al., 2024). Key parameters affecting the nucleation and growth rate of the ice layer include the degree of supercooling (how much the temperature is below the freezing point), the presence of impurities or catalysts that can facilitate nucleation, and the surface energy, which determines how easily water molecules can align to form ice. Once nucleation has begun, the growth rate of the ice layer is influenced by factors such as ambient temperature, heat transfer properties of the surface, and the availability of water molecules. These factors collectively determine how quickly and extensively ice forms on a given surface(Makkonen, 1984; Makkonen & Stallabrass, 1984).

The transformation of an ice deposit into a cylindrical ice shape on a cable is primarily governed by the mechanical and thermal interactions between the ice and the cable. As ice accumulates on the cable, it initially forms a less-defined, irregular shape. However, as the deposit grows, gravitational forces and the cable’s curvature cause the ice to compress and

redistribute itself into a more uniform, cylindrical form. This shape is further stabilized by the mechanical stress imposed by the weight of the ice and the surface tension effects, which work to minimize the surface area in contact with the cable. Additionally, thermal gradients and the temperature variations can lead to differential melting and refreezing, contributing to the development of a cylindrical profile.

Shedding refers to the process by which an ice layer detaches from a surface after nucleation and growth. This detachment can occur naturally due to various factors, such as changes in temperature, mechanical vibrations, or wind forces(Druez et al., 1995). Shedding is crucial in applications where ice accumulation can cause problems, such as on aircraft wings, power lines, or wind turbines. The effectiveness of ice shedding depends on the adhesion strength between the ice and the surface. Factors such as surface roughness, material properties, and the presence of hydrophobic coatings can significantly influence the ease with which ice detaches. For example, surfaces designed to minimize ice adhesion, often through special coatings or textures, can promote quicker and more complete shedding. Temperature plays a vital role as well; warming the surface or the surrounding air can reduce the adhesion force, making it easier for the ice to slide off (Solangi, 2018).

Prediction of ice accumulation is basically referring to the persistent step where ice is in the persistent step and has a cylindrical shape. A list of ice prediction models and their application based on the ice type (rime, wet snow, or glaze) are provided in Cigré (Cigré, 2006). However, there is another classification for ice prediction models (M. Shabani et al., 2022). The ice prediction models are divided into three main groups, namely physic-based model, observational/experimental-based models, and probabilistic-based models.

International Standard Organization (ISO) suggests the proposed model by Makkonen (Makkonen, 2000) that is based on the heat balance equation. The model has a complex structure; however, its prediction is quite accurate and precise. CSA C22.3 recommends employing the Chaîné and Castonguay(Chainé & Castonguay, 1974). It is developed based on

the assumption of freezing all impinged drops on the surface. The model assumes that the iced conductor has an elliptical shape and introduces a correction factor. An empirical model for computing of the correction factor based on ambient temperature and radius of rod can be found in literature (Stallabrass et al., 1967). The most challenging issue in the model is the dependency of the model on the radius of conductor and estimation of correction factor. Jones in a comprehensive study showed that this model overestimates ice accretion and may not be effective (Jones, 2023). This model also ignores the effect of run-off and bouncing. In addition, the model neglects the fact that all drops cannot necessarily stick to the surface due to several factors, such as wind speed. CRREL model, which is one of the mostly used empirical models, is developed based on the assumption of collision efficiency is 100%(Jones, 1996a). In other words, if a supercooled drop does not bounce and could stick to the impinged surface, it will freeze completely. Another model could be the Goodwin model is develop based on the assumption that all supercooled drops freeze on the impinged surface and neglects the effect of bouncing and runoff (Goodwin et al., 1983).

1.5 Performance based engineering

Traditional design approaches in engineering relied heavily on prescriptive codes and standardized safety factors, which dictated specific design requirements without considering the unique performance needs of each structure. These methods provided a one-size-fits-all solution that often led to overdesign or inefficiencies, as they didn't account for the actual demands a structure might face during extreme events. The main problems with these approaches were their inability to accurately predict structural behavior under varied conditions and their lack of flexibility in accommodating new materials or innovative design techniques. This resulted in designs that were either unnecessarily conservative or insufficiently robust, potentially compromising safety and cost-effectiveness.

Performance-based engineering (PBE) is an advanced approach to structural design that focuses on achieving specific performance goals under various loading conditions. PBE was

primarily designed and applied for risk assessment of structures subjected to earthquake threat (Porter, 2003). Unlike traditional methods that follow prescriptive codes, PBE allows engineers to tailor designs to meet predefined performance objectives, such as minimizing damage during an earthquake or maintaining functionality during extreme weather events(Ciampoli et al., 2011). This approach uses detailed analytical techniques, including nonlinear dynamic analysis, to predict how structures will respond to different hazards. By doing so, PBE enables the identification and strengthening of vulnerable areas in a structure, ensuring that it can withstand the anticipated demands. PBE also considers life-cycle costs, allowing for a more comprehensive evaluation of the trade-offs between initial investments and long-term benefits, such as reduced repair needs after an event(Barbato et al., 2013). It has been successfully applied in the design of buildings, bridges, and infrastructure in seismic zones, where safety and resilience are critical. As PBE continues to evolve, it plays a vital role in the development of performance-based codes and standards that accommodate new materials and construction techniques. Ultimately, PBE promotes more resilient and optimized structures, aligning engineering practices with modern challenges and societal needs.

The first PBE framework that was proposed by Pacific Earthquake Engineering Research (PEER) had four modules (see Figure 1.3).

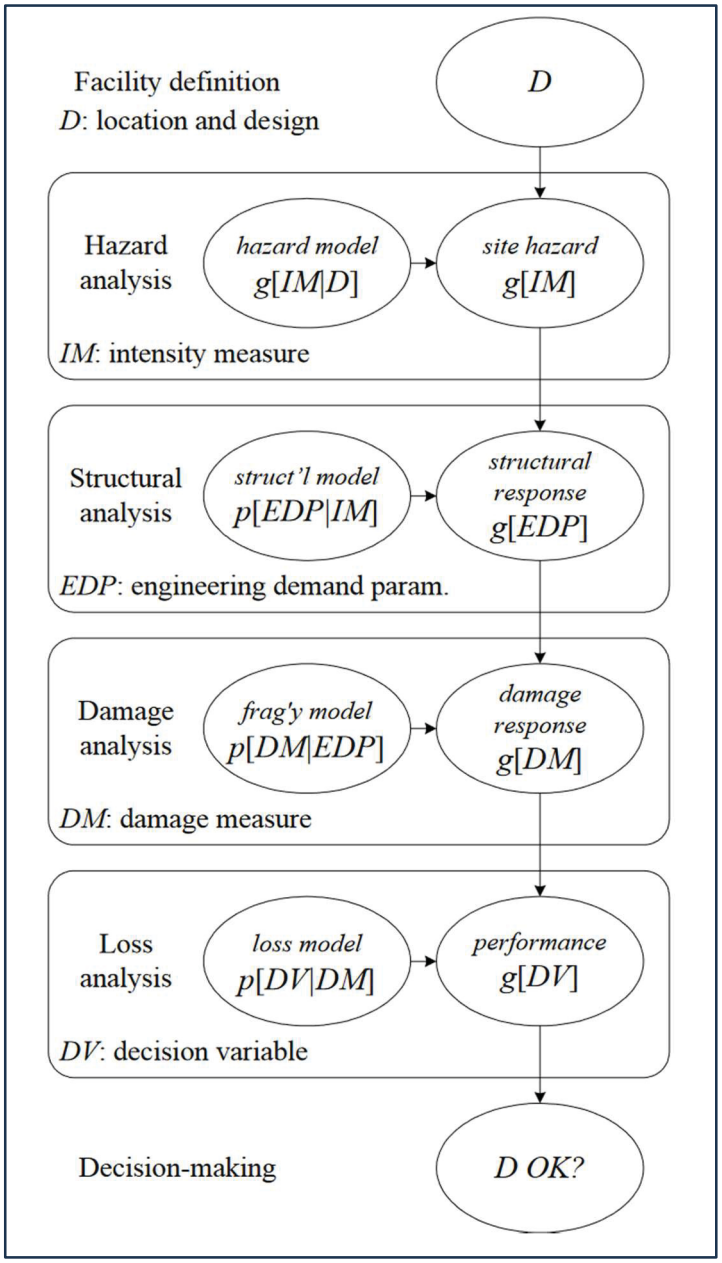

Figure 1.3 The PBE proposed by PEER
Taken from (Heresi & Miranda, 2023)

During the last decades, PBE has been flourishingly employed for prediction of the potential threat of different hazards and has been upgraded consequently. For instance, several studies have been carried out to identify the most important Structural Parameters (SP) affecting the structural risk (Herbin & Barbato, 2012; Y. Li & Ellingwood, 2006). Ciampoli introduced

another module to the PEER's proposed framework, namely "interaction analysis" that accounts for more interaction of different hazards. For instance, one of the interactions during freezing rain events is wind actions and ice accumulation simultaneous impact that can be translated as the change in drag and lift coefficients. Barbato(Barbato et al., 2013) promoted the framework to account for multi hazard events and applied for prediction of hurricane threat. Similarly, the effect of time varying factor in loss analysis was considered (Esmaeili & Barbato, 2022) using constant interest rate. Several other examples can found in the literature where applied PBE for different threats, such as fire(Buchanan, 1994), wind(Augusti & Ciampoli, 2008; Ciampoli & Petrini, 2012). Although numerous studies have been conducted for prediction of risk in different subfields, few research has been carried out in the era of ice engineering. For instance, Snaiki and Shabani(Snaiki & Shabani, 2023) developed a novel multi-scale PBE for risk assessment of ice storms. Notably, it is of great importance to dig deeper and apply the PBE principles for freezing rain events. However, as previously mentioned, freezing rain events have some challenges, such as intensive computational cost associated with performing the risk assessment at extensive scale, time-varying climatological patterns that makes prediction challenging more than ever, and the complexity of accurate estimation of ice characteristics during accumulation and shedding steps.

1.6 Machine learning algorithms

Machine Learning (ML), which is a field of artificial intelligence (AI), is used for extracting the information from a given dataset (Brunton et al., 2020). Generally, ML models are classified into four main groups: (1) supervised learning; (2) unsupervised learning; (3) semi-supervised learning; and (4) reinforcement learning (see Figure 1.4). Among them, Artificial Neural Network (ANN), which is a supervised learning ML model, has been extensively used for both classification (e.g., (Chang et al., 2016)) and regression (e.g., (M. Shabani et al., 2022)).

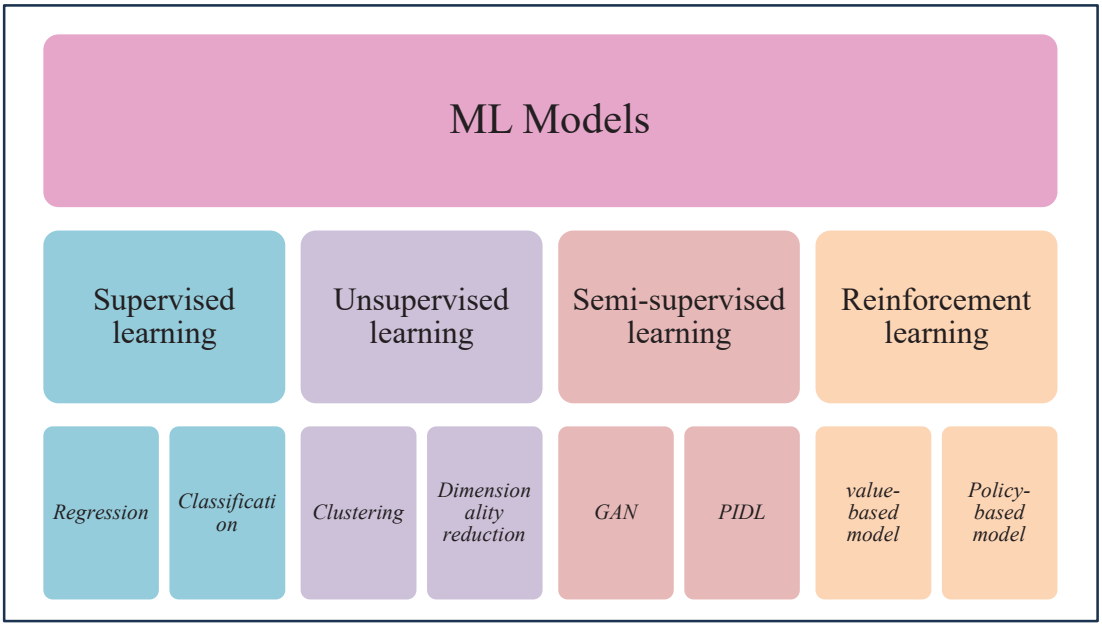

Figure 1.4 ML classification

ANNs are numerical models, which are inspired by the structure and function of the human rain, particularly the way neurons are interconnected to form a complex network. ANNs have been successfully applied to a broad range of civil engineering subfield (e.g., ice engineering) where they can be used to predict characteristics of the natural hazard (e.g., (Yue Ming, 2018)) and estimate their corresponding loads on structures (e.g., (P. Li et al., 2010)). An ANN architecture typically has three main layers: 1 input, 2. hidden, and 3 output. The input layer receives the input data, with each node representing a feature or attribute of the data. The hidden layer performs computations that enable the network to learn from the input data through backpropagation, adjusting the weights and biases of the neurons. The output layer generates predictions of the network based on the information learned, with each output node representing a class or category that the network is trained to predict. The process of learning basically includes five consecutive steps: (1) collecting the data; (2) data preparation; (3) training the model; (4) evaluating the model's performance; and (5) hyperparameters tunning (Wu & Snaiki, 2022). Conventional ANNs integrate backpropagation optimizer within their learning mechanism because of its advantages. The backpropagation algorithm (Rojas, 1996) updates the networks parameter through optimizing the predefined loss function. The updating

of the unknown parameters continues until the defined stopping criterion is fulfilled (e.g., maximum number of iterations, early stopping, gradient threshold, and convergence of loss function). The ANNs have been widely employed in different studies (e.g., (Ogretim et al., 2006)) to address some of issues of ice accretion process, such as albeit complexity of accumulation process, significant discrepancy of empirical ice models, and lack of generalizability of empirical models. Therefore, they can be integrated with in the framework to address the issue of computational cost for obtaining the Engineering Demand Parameters (EDP) and Damage Measures (DM). Moreover, they can be alternatively employed for describing the complex interaction of different hazards during freezing rain events. For instance, a Feed Forward Neural Network (FFNN) was trained based on reproduced data obtained from icing wind tunnel test to eliminate the need for performing extremely expensive numerical analyses (Snaiki & Shabani, 2023).

1.7 Internet of Things

The Internet of Things (IoT) is a network of physical devices embedded with sensors, software, and other technologies that connect and exchange data over the internet. These devices, often referred to as "smart" objects, can range from everyday household items to complex industrial machinery. The primary goal of IoT is to create a seamless flow of information between the physical and digital worlds, enabling real-time monitoring, automation, and decision-making(Scuro et al., 2018). IoT's impact on environmental monitoring and real-time prediction is profound. By leveraging IoT devices, organizations and governments can collect and analyze environmental data on an unprecedented scale, leading to more informed decision-making and proactive measures(Deak et al., 2013). IoT leverages the potential of several technologies advancements, such as sensor technology, wireless communication, cloud computing, and ML. IoT plays a significant role in enhancing weather prediction accuracy and understanding climate change by providing a vast network of data collection points and enabling real-time analysis. For instance, IoT devices, such as weather stations, buoys, and satellites, are equipped with sensors that continuously monitor atmospheric conditions like temperature, humidity,

wind speed, and barometric pressure. This data is transmitted in real-time to central systems where it is processed using machine learning algorithms to generate accurate weather forecasts. By integrating data from numerous IoT devices across the globe, meteorologists can predict weather patterns with greater precision and issue timely warnings for extreme weather events such as storms, floods, and heatwaves. In addition, IoT is instrumental in studying and mitigating the effects of climate change. Sensors deployed in various ecosystems—such as forests, oceans, and polar regions—collect data on temperature, CO_2 levels, ice thickness, and sea levels. This continuous stream of data helps scientists track variation in the environmental parameters, identify trends, and model the impacts of climate change. For example, IoT-enabled devices can monitor the melting of polar ice caps and rising sea levels, providing critical information for climate models and helping to predict future scenarios.

1.8 Summary

The chapter discussed the freezing rain characteristics, its associated challenges in development of a spatial-scale risk predictive model. Moreover, it compared the problems in accurate estimation of ice shape and studied the instabilities during freezing rain event. In addition, it explored the PBE principles, its application and development to different subfields and its limitations in development of a Performance-Based Freezing Rain Engineering (PBFRE) framework for real-time prediction of freezing rain-induced risk to transmission networks, especially the conductors. Additionally, it showcased the potential of ML and IoT in addressing the issues of PBFRE framework for spatial and structural scale.

CHAPTER 2

RESEARCH METHODOLOGY

2.1 Introduction

In order to investigate the feasibility of PBE principles for estimating the freezing rain-induced risk and make a meaningful contribution to the PBE development and application, this study aims to explore to figure out the freezing rain challenges and its corresponding problems in design and implementation of an automated performance-based design mechanism and development of an early warning system in order to mitigate the potential risks during freezing rain events.

The decision to employ PBE is grounded in the need for a design approach that aligns with the specific performance objectives and environmental challenges inherent to our project. Unlike prescriptive code-based methods, which often impose generalized criteria, PBE offers a tailored framework that directly addresses the unique demands of infrastructure systems (Dorri et al., 2023).

PBE enables the customization of design parameters to the unique operational and environmental conditions of the project. This approach allows for a more precise alignment with the anticipated load cases and usage scenarios, ensuring that the system's performance meets the exact requirements rather than relying on generalized safety margins.

By focusing on the actual performance of the structure under various potential scenarios, including extreme events, PBE enhances the resilience of the system. This is particularly critical in our case, where the infrastructure must withstand specific environmental stressors, making it essential to evaluate and mitigate risks comprehensively. In addition, the PBE framework's inherent flexibility encourages the exploration of innovative design solutions that

may not conform to traditional standards. This flexibility is crucial in our project, where novel approaches are required to meet unique performance criteria.

2.2 Steps in developing the framework

The main steps in developing a meaningful solution for automated and accurate risk estimation of freezing rain-induced risk are: (1) defining the performance objectives; (2) understanding the source uncertainties during freezing rain events; (3) defining of the risk problem; (4) solve risk problem and estimate the structural risk; (5) identification of the framework's limitations in application at structural and spatial scales; and (6) exploring the potentials of IoT and ML in addressing the problems and obstacles in the path of real-time freezing rain risk estimation. Figure 2.1 depicts the main steps in achieving the best and optimized solutions for attenuating the freezing rain-induced risk.

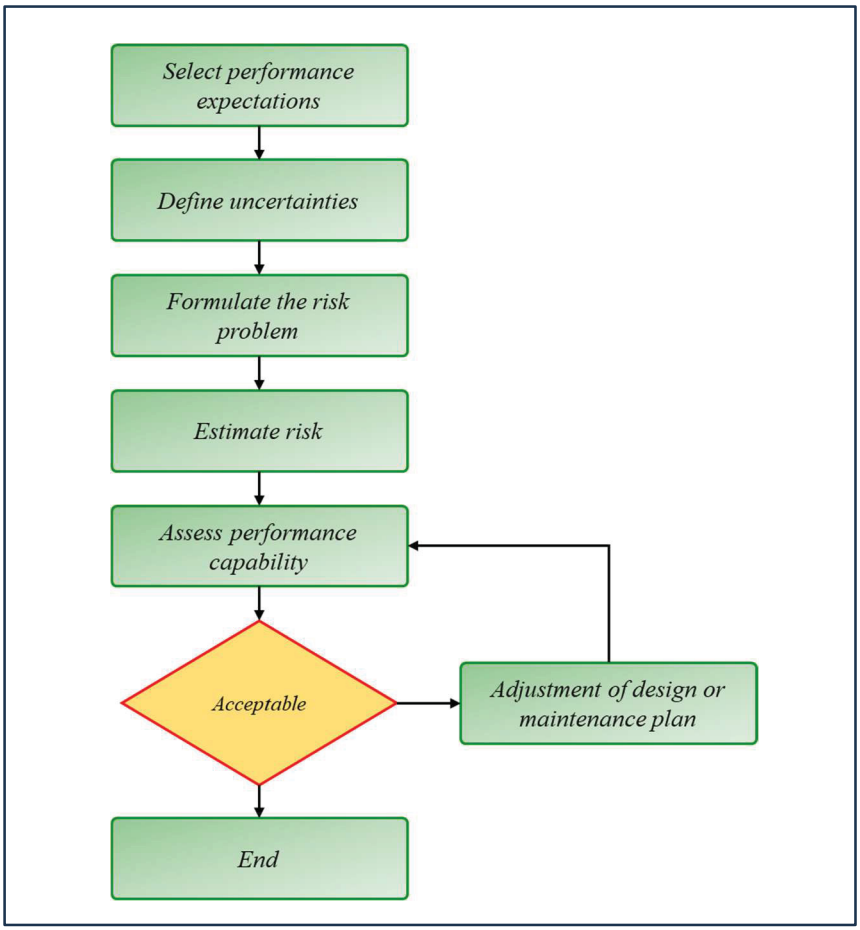

Figure 2.1 Steps involved in optimizing the design and maintenance plan of a system prone to freezing rain

2.3 Research motivation

Freezing rain events prevail an extensive area in northern countries every year and cause severe damage to infrastructures. For instance, during north American ice storm 1998 in Quebec, there was a quite fundamental damage to the electrical grid. More than five million customers had to spend days without electricity and heat in cold weather. In total, the storm caused three million dollars in lost and death of dozens.

Developing a PBE framework for structural systems prone to freezing rain events is crucial due to the unique and severe challenges posed by such conditions. Freezing rain can lead to significant ice accumulation, increasing the loads on structures and potentially causing failures.

Traditional methods for risk assessment and mitigation often fall short in capturing the complexity and variability of these events, especially under changing climate conditions.

One of the primary reasons for advancing a PBE framework is to provide a more accurate and tailored approach to assessing and managing the risks associated with freezing rain. However, solving the risk problem within this framework is computationally intensive. The stochastic nature of freezing rain events, combined with the need to model the structural response under various scenarios, significantly increases the computational cost. This challenge is further exacerbated when real-time prediction and decision-making are required, a critical aspect that has not been adequately addressed in many existing studies.

To overcome these limitations, our study integrates ML and IoT technologies into the PBE framework. ML algorithms can efficiently process large datasets and identify patterns that may not be evident through traditional methods, enhancing the accuracy of predictions. The IoT provides real-time data acquisition from sensors monitoring environmental conditions and structural responses, enabling dynamic updates to the risk assessment model. This combination not only reduces the computational burden but also allows for more effective real-time prediction and management of freezing rain risks, making the PBE framework more robust and applicable in practical scenarios.

The integration of IoT and the leverage of Machine Learning within this framework further amplifies these benefits. IoT devices provide real-time monitoring of both environmental conditions and structural responses, offering critical data that can be used to update risk assessments dynamically. This continuous flow of information ensures that the PBE framework remains responsive to actual conditions, enhancing its accuracy and reliability. Machine Learning, on the other hand, enables the analysis of vast amounts of data to identify trends, predict future events, and optimize decision-making processes. Together, IoT and Machine Learning not only improve the precision and adaptability of the PBE framework but

also pave the way for proactive maintenance strategies and real-time risk mitigation, ultimately leading to safer and more resilient infrastructure in the face of freezing rain events.

2.4 Research questions

The major problem that is addressed in this study is application of PBE for risk estimation of structural systems and infrastructures where are subjected to freezing rain events and suffer from their corresponding side effects. Moreover, other issues which are not addressed become a source of motivation to accelerate the research. For instance, the climate change effects are becoming increasingly an important matter since it affects the rate and patterns of precipitations and alters the temperature which is a key factor in nucleation and accumulation processes. Based on the gaps found in the literature, issues located in the industries, the major research questions in this study are as follows:

1. How PBE can contribute to better designing of structural systems in cold regions?
2. How PBE can be designed and implemented in an extensive area while providing accurate and quick predictions of freezing rain-induced risk.

To respond to the first question, a comprehensive review on the literature review is conducted to showcase the effectiveness of the PBE in attenuating the risk of hazards (e.g., earthquake) to structural systems. The stats demonstrated the superiority of PBE over other design approaches.

To answer the second question, the PBE framework is developed based on the total probability theorem and its modules are defined based on the potential threats during a freezing rain event. Its application is illustrated at two times throughout lifecycle of an electrical grid: (1) early design steps and (2) maintenance planning. The risk problem is formulated at two scales: (1) structural and (2) spatial. The first paper in chapter (3) explains the definition, analyses and

comparison of the results. In the second paper, application of a novel ML for prediction of ice accretion in cylindrical shape is showcased.

2.5 Research objectives

The comprehensive literature review demonstrated few studies conducted for development and improvement of PBE in prediction of structural risk of infrastructures prone to freezing rain threat. As a results, the main objective of the current study is to apply PBE principles for facilitating the risk problem of an iced system. Specifically, the domain of the current study is restricted to freezing rain events and cannot be applied for other types of atmospheric icing, such hard rime. Notably, given the limited literature on application of PBE for freezing rain, the challenges for development are detected and addressed through leveraging the capabilities of ML algorithms and IoT principles.

2.6 Publications

To enhance clarity, this thesis is divided into one article, and the next section presents brief summaries of this article.

2.6.1 Paper 1: A Novel Performance-Based Framework for Freezing Rain Events (Journal paper that is under review)

This article is considered as the core of the thesis as it explains the implementation of PBE for prediction of freezing rain-induced risk for vulnerable systems in cold regions. It is specifically concerned about the challenges of applying PBE for estimation of freezing rain-induced risk and spatial scales while providing accurate and online predictions. Notably, this en submitted to the Structural Safety journal.

CHAPTER 3

A NOVEL PERFORMANCE-BASED FRAMEWORK FOR FREEZING RAIN EVENTS

Mahdi Shabani, Michel Kadoch[1]

[1] École de technologie supérieure, Montréal, Canada

Paper submitted at *Structural Safety Journal*, August 2024

3.1 Abstract

Freezing rain is one of the most damaging natural hazards that interrupts the integrity of infrastructures in cold regions during winters or springs. Therefore, accurate and computational efficient prediction of freezing rain-induced risk is compellingly crucial and required for design and assessment of structural systems. However, there are numerous issues associated with forecasting of freezing rain, including extensive multi-hazard nature, computational cost, unpredictable, and complexity. Therefore, an innovative high-level and advanced performance-based decision-making framework is presented to address some of the issues. The proposed framework is innovatively capable of accounting for the variability of climatological patterns due to climate change effects while addressing the issue of computational cost for facilitating an automated risk-informed decision-making framework. The novel high-level framework improves design of new structural systems which are exposed to freezing rain and optimizes the rehabilitation plans for promoting their resiliency. Additionally, the advanced multi-scale, performance-based framework exploits the capabilities of advanced predictive models and internet of things principles to predict the extreme freezing rain-induced risk not only efficiently but also accurately. Application of the proposed structural system is illustrated through risk assessment of an iced transmission line at two parts, namely maintenance and

design in two scales. The novel high-level framework can be conveniently integrated into a wide range of predictive systems (e.g., early warning systems or manless mitigation systems) so that they can save life of thousands, keep the infrastructures operational and minimize the freezing rain-induced cost in cold regions.

Keywords: Ice, Machine learning, Performance-based engineering, risk; real-time

3.2 Introduction

Freezing rain, typically characterized by supercooled raindrops that freeze immediately upon impact, accounts for significant damage to infrastructures in middle and high-latitude societies (see Figure 3.1). It is generally observed when a cold layer of air is covered by a warm mass of air that eventually results in forming an ice crust on exposed surfaces, such as transmission lines (Kämäräinen et al., 2018). The length of warm front (H_{max}- H_{min}) dictate the characteristics of supercooled drops. The major problem in freezing rain events is the accumulated accreted ice coats that causes several adverse effects in residential areas (e.g., traffic due to reduced friction, depression of societies due to power outage, and even human injuries or human death) and non-residential areas (e.g., fallen trees, road blockage).

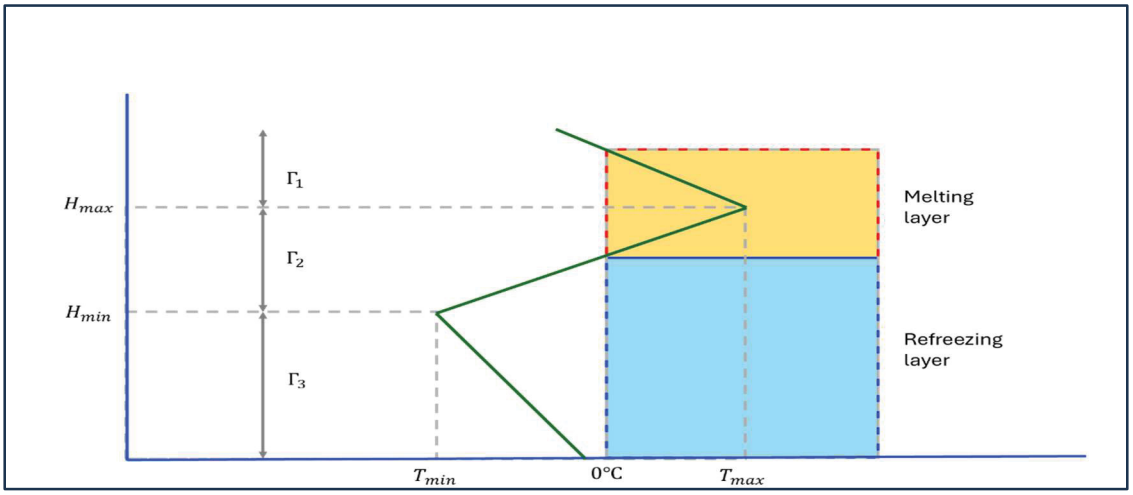

Figure 3.1 Conceptual model for characterizing the required condition for occurring freezing rain event

If moderate wind blows, the ice-induced risk could be exacerbated through onset of wind-induced instabilities that compromise the integrity of iced structural systems(K.F. Jones, 1996). Numerous reports on devastating freezing rain-induced risk to residential communities can be found in the literature. For instance, the North American 1998, a massive combination of five successive ice storm, prevailed parts of Canada and United States, caused power outage of five million customers and two billion dollar lost for Quebec alone and several fatalities (Lecomte et al., 1998). Another example could be 5th April 2023 ice storm that devastated Ontario and Quebec, caused power outage of more than one million customers and $3 billion of damage. Freezing rain events typically prevail over an extensive geographical area, they could potentially impact the integrity of every single vulnerable structural system to ice accretion (e.g., wind turbines and cable-stayed bridges). For example, Wachusett Wind Turbine experienced structural failure due to formation of approximately 2-inches of glaze ice in November 2002. In total, freezing rain events are responsible for about 20% loss of energy production on wind farms(Jasinski et al., 1998; Wallenius & Lehtomäki, 2016). Moreover, they are responsible for millions of dollars loss due to power outage of transmission systems in northern countries. In addition, climate change which is a result of deforestation, industrialization, agricultural modernization, and cities development has already altered the climatological patterns that will ultimately impact frequency and intensity of precipitation. As a result, the conventional approaches cannot be applied for accurate estimation of freezing rain-induced risk to residential/non-residential areas. Consequently, it is crucial to develop innovative advanced methodologies that ensures optimized design and effective maintenance of structural systems prone to freezing rain and facilitate immediate and accurate estimation of freezing rain-induced risk across extensive geographical regions.

Performance-Based Engineering (PBE) framework which was initially designed for seismic engineering applications can conveniently supersede conventional risk approaches (e.g., allowable stress design and load-and-resistance-factor design) in one or many forms(Porter, 2003). The articulation of performance metrics is the key factor for this selection. However,

possessing a profound understanding of intensity measures (i.e., environmental threats), structural components (i.e., structural parameters), interaction between the structure and its surroundings environment, and anticipated performance objectives is crucial for implementation and development of a PBE methodology in order to maintain/mitigate the hazards-induced risks at a level in which the structural system can achieve the predetermined performance levels and perform as intended (Yu et al., 2020). In general, PBE procedures are established based on the proposed framework by Pacific Earthquake Engineering Research (PEER)(Heresi & Miranda, 2023) based on total probability theorem. PBE has been successfully applied to various subfields of engineering disciplines, such as Performance-Based Wind Engineering (PBWE)(Ciampoli et al., 2011; Ouyang & Spence, 2021; Wu et al., 2024), Performance-Based Hurricane Engineering (PBHE) (Barbato et al., 2013; Cui & Caracoglia, 2018; Esmaeili & Barbato, 2022), Performance-Based Fire Engineering (PBFE) (Rini & Lamont, 2008; Su et al., 2021), Performance-Based Tsunami Engineering(PBTE) (Attary et al., 2021; Behrens et al., 2021), and Performance-Based Seismic Engineering (PBSE) (Chandler & Lam, 2001; Heresi & Miranda, 2023), among others. Although plenty of studies can be found in different disciplines, there are few studies revealing the potential applications of PBE in snow/ice engineering subfield. For instance, Liel et. al (Liel et al., 2011) employed the proposed framework by PEER for risk assessment of snow on envelopes. The proposed performance-based snow engineering includes four main modules, namely hazard analysis, structural analysis, damage assessment, and loss and risk analysis. The application of the framework was illustrated through risk assessment of a building in Colorado. Another example could be the study of Snaiki (Snaiki, 2024) that developed a Performance-Based Ice Engineering (PBIE) for estimation of ice storms-induced risk on structural systems. The study illustrates the application of PBIE for risk assessment of a one-inch diameter iced conductor in Quebec based on linear theory of suspended cables(H. M. Irvine & T. K. Caughey, 1974). However, few studies can be found in the literature that account for the effect of variability of climatological patterns and have provided effective plans to address the freezing rain associated issues, including multi-hazard, complexity of the accumulation and variability of

climatological patterns. In addition, there are few studies that demonstrated how to employ PBE principles for maintenance and design of structural systems prone to freezing rain events.

In this study, an innovative advanced performance-informed freezing rain framework based on the PEER framework will be developed for accurately and efficiently estimation of freezing rain-induced risk on structural systems at both design and maintenance steps. Specifically, the proposed framework addresses issues of previous frameworks by leveraging the capabilities of Internet of Things (IoT) and Machine Learning (ML). The framework will be developed based on the total probability theorem and can be disaggregated into some modules, namely hazard analysis, structural characterization, interaction analysis, structural analysis, damage analysis, loss analysis and decision making. A description of each module will be presneted. The application of the framework will be illustrated through risk assessment of tower-line transmission system prone to freezing rain at two scales: structural and spatial. Specifically, the potential risk of galloping onset due to combined effect of wind actions and glaze ice accumulation will be studied. In the local scale, Finite Element (FE) model will be developed to study the dynamics of tower-line transmission system prone to freezing rain. Then, the study will leverage the potential of an advanced surrogate model (Sparse Identification of Nonlinear Dynamics(Brunton et al., 2016)) to address the issue of intensive computational. In the spatial scale, historical spatiotemporal climatological observations will be retrieved from Automated Surface/Weather Observing Systems (ASOS). To investigate the effect of different empirical freezing rain prediction models on extreme map, several models, namely Chaine and Castonguay(Chaîné & Castonguay, 1974), Goodwin et al.(Goodwin et al., 1983), the Cold Regions Research and Engineering Laboratory (CRREL) simple model(Jones, 1996a; Jones et al., 2004) will be employed for predicting total hourly accumulated glaze ice. Advanced statistical analyses based on extreme value theory(Nygaard et al., 2014) will be carried out and spatial interpolation using Ordinary Kriging (OK)(Johnston et al., 2003) with nugget nonzero will be performed. Feature selection (geospatial parameter) will be carried out based on total Sobol indices acquired from polynomial expansion(Crestaux et al., 2009) to identify the relationship between geographical parameters and residual values obtained from spatial

interpolation. A metaheuristic-based Feedforward Neural Network (FNN) will be fitted for estimation of residuals across the domain and adjusting the estimations. The concurrent wind speed will be computed based on the proposed approach by Jones et. al(Jones et al., n.d.). Moreover, the IoT principles will be utilized for prediction of freezing rain-induced risk and a comparison will be carried out.

3.3 Proposed framework

This study develops and introduces an innovative framework for real-time freezing rain-induced risk assessment to contribute to Benefit-Cost Ratio (BCR) optimization of structural systems in cold environments. The proposed framework is applicable to two scales: (1) structural scale and (2) spatial scale. In the former, the integrity of a structural system prone to freezing rain is assessed and contributes to decision-making regarding the structural system. In the latter, the proposed framework is employed for identification of vulnerable parts across an extensive region and prevent potential threats. Since the PBE is developed based on total probability theorem, it is crucial to understand the sources of uncertainties and performance objectives. Therefore, a review on uncertainties and performance objectives of freezing rain events is provided in section 2.1.; following that, the framework modules in two scales (i.e., structural and spatial) is elaborated.

3.3.1 Sources of uncertainties & performance levels

3.3.1.1 Freezing rain loads and effects

Depending on several environmental factors (e.g., rate of precipitation, wind speed, humidity, and exposure), surface characteristics (e.g., roughness, dimension, material and moisture), and particle dimension, accumulated ice characteristics could be different (Makkonen, 2000). During a freezing rain event, there might be several thermodynamic, hydrodynamic, or aerodynamic processes. Specifically, the current study is exclusively concerned with the

interaction between wind actions and supercooled drops/accumulated ice. According to investigation of Hydro Quebec in January 1998, the combined effect of wind actions and ice accumulation had triggered the collapse of specific ground wires and conductors and attributed to cascading (Goel, n.d.). Consequently, wind-induced loads on iced structures and the vertical load due to accumulated ice weight are the most important loads during freezing rain events. Ideally, wind speed at different heights can be disaggregated into two components: mean wind speed and turbulent component. Although actual mean wind speed is higher than estimations within boundary layer, it is deemed that power and logarithmic laws can represent mean wind speed. Regarding turbulent component, computing statistical parameters from historical wind measurements and predicting using statistical methods are recommended (Snaiki, 2024). Wind-induced vibrations are classified as aeolian vibrations and wake-induced oscillations can impair integrity and reliability of structures prone to ice accumulation (Van Dyke et al., 2008a).

Galloping, as a motion-induced excitation, is typically characterized as high-amplitude and low-frequencies oscillations. The onset and development of galloping oscillations in transmission lines are primarily driven by aerodynamic instability, often initiated under specific environmental conditions such as the presence of ice or snow accretion on the conductors. As wind flows across the irregularly shaped ice deposits, it generates lift forces that exceed the restoring forces of gravity and tension, causing the line to oscillate (see Figure 3.2)(Hartog, 1932). These oscillations typically begin at low frequencies and can amplify rapidly if the aerodynamic forces continue to drive the motion, leading to large amplitude oscillations. The development of galloping is influenced by factors such as wind speed and direction, conductor tension, ice shape and distribution, and the mechanical properties of the transmission line system. The galloping mechanism has been studied and predicted using an empirical model (e.g., (McComber & Paradis, 1998)) or data-driven one (e.g., (Liu et al., 2023; Lu et al., 2019)). The ice load can be seen as extra dead load due to the weight of the ice coat. Estimation of the ice coat thickness is typically done by either explicit ice accretion models (e.g., Chaîné and Castonguay(Chaîné & Castonguay, 1974), CRREL(Jones, 1996b), and ISO 12494(Makkonen, 2000)) or field observations (e.g., electronic sensors, load sensors,

cameras(Gou et al., 2023)) and represented in cylindrical shape. However, wind-induced instabilities onset once an asymmetrical layer of ice forms on the surface. These dynamic effects are challenging to characterize and are often not accounted for in the design codes or standards. To avoid such difficulties, codes and design practices proposed overly conservative assumptions based on radial ice deposit to cover the wind-induced oscillations. However, they cannot necessarily guarantee the integrity of iced structural systems in cold sessions.

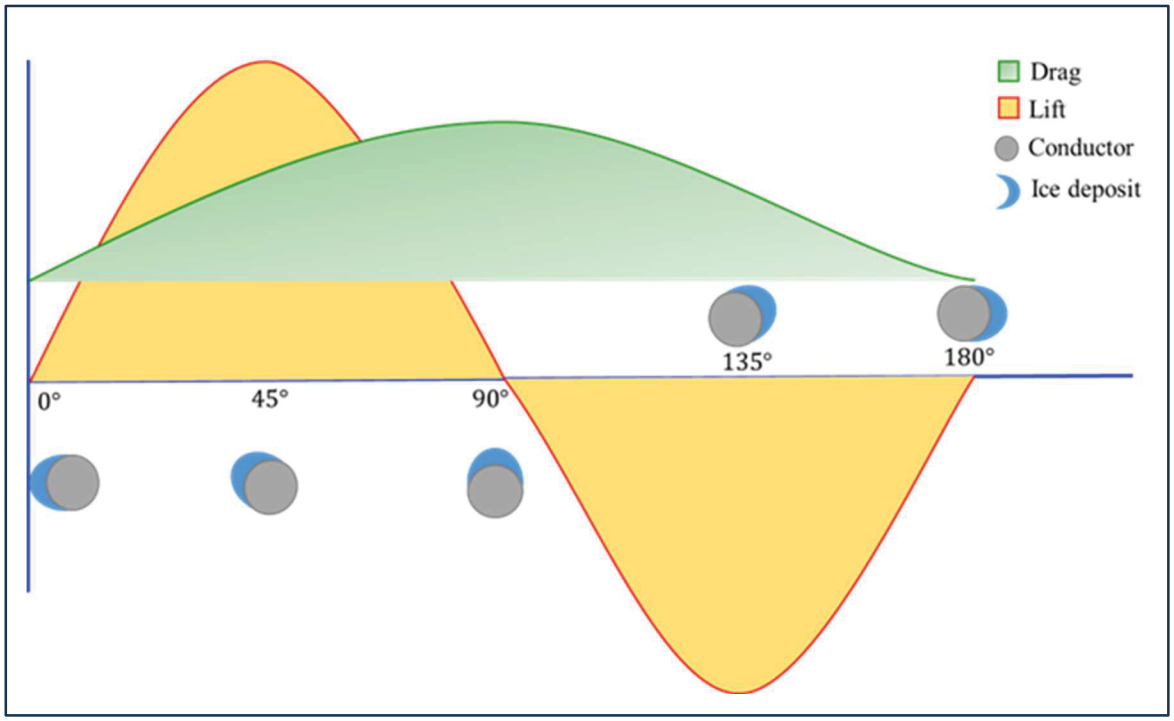

Figure 3.2 Variation of lift and drag coefficients with respect to angle of attack

Theoretically, onset and development of galloping oscillations requires fulfilling three criteria: (1) negative Den Hartog coefficient, (2) wind speed surpass critical wind speed, and (3) negative total system damping (Davalos et al., 2023). The first criterion (i.e., Den Hartog coefficient(Hartog, 1932)) can be estimated using Eq. (3.1) .

$$a_g = C_d + \frac{dC_l}{d\alpha} \tag{3.1}$$

wherea_g= Den Hartog coefficient, C_d = drag coefficient, C_l = lift coefficient, and α = Angle of Attack. Several experimental studies can be found in the literature (e.g., (Rossi et al., 2020)) that the area in Figure 3.2 indicating negative Den Hartog coefficient have been highlighted. If free stream wind speed exceeds the critical wind speed (see Eq. (3.2)), there is a high chance of instability occurrence (SCRUTON & FLINT, 1964).

$$f = V - V_c \tag{3.2}$$

$$V_c = \frac{2.S_c.f_n.d_c}{a_g} \tag{3.3}$$

where S_c = Scruton number, f_n = natural frequency, and d_c = the diameter of bare conductor. For simplicity, from now on, "diameter" refers to the diameter of bare conductor. Galloping can fully develop once the total system damping, ξ, becomes negative (see Eq. (3.4)).

$$\xi = \xi_s + \xi_a < 0 \tag{3.4}$$

where ξ_s = structural damping and ξ_a = aerodynamic damping. Generally, the majority of studies employ the simplified linear theory(H. M. Irvine & T. K. Caughey, 1974) for characterizing the dynamics of transmission line. The validation of the theory is restricted to sag to span ratio of 1:8 and less. The symmetric in-plane mode shape of a transmission line, as the most govern mode in describing galloping movements, can be described as

$$\varphi_n(x) = 1 - \tan\left(\frac{1}{2}\beta_n L\right)\sin(\beta_n x) - \cos(\beta_n x) \tag{3.5}$$

$$\omega_n = \beta_n.\sqrt{\frac{H}{m_s}} \tag{3.6}$$

Where, φ_n = nth symmetric in-place mode shape, L = span length, ω_n = natural frequency of nth mode, m_s = mass of bare conductor, and H = horizontal component of conductor's tension. Eq. (3.5) cannot be solved explicitly, and numerical approaches should be employed. Several effective parameters in Eq. (3.5) are not determined accurately and might have uncertainty.

3.3.1.2 Uncertainties characterization

There are a wide variety of classifications for uncertainties in a problem, but Kiureghian (Der Kiureghian, 2022) classifies them into two main groups, namely epistemic (aka systematic or reducible uncertainty) and aleatoric (aka statistical or irreducible uncertainty). Epistemic uncertainties include modelling errors, incomplete data, and parameter uncertainty, whereas aleatoric uncertainties encompass randomness in measurements and intrinsic variability in the system. Similar to previous studies (e.g., (Barbato et al., 2013; Ciampoli et al., 2011; Snaiki, 2024; Snaiki & Shabani, 2024)), the uncertainties sources in the risk estimation problem are: 1. the environment zone, 2. the exchange zone, and 3. the structural zone. In the environment zone, hazard intensities are assessed without accounting for the interference effects of structures. However, interactions between the hazards may occur, potentially complicating the assessment of the associated uncertainties. In the "exchange zone", this region surrounds the system, where the hazard and the system exhibit a high degree of correlation. Within this zone, the interference effects caused by the presence of nearby structures are also significant. The latter implies real-time characteristics of the target structural system (e.g. tower-line transmission system). The manufacturing and assembly errors, impact of degradation, and third-party activities can be considered in this zone. It is of great importance to note that this study does not cover epistemic uncertainties; however, the proposed framework is flexible enough to account for epistemic uncertainties as well.

3.3.1.3 Performance expectations

Performance expectations are conventionally determined by assessing hazard(s)-induced damage (structural and non-structural ones) and the corresponding losses and quantified in terms of tolerable damage. They are basically a function of several factors, including nature of the hazard, type of structural system, and presence of non-structural elements(Esmaeili & Barbato, 2022; Mackie et al., 2009). Previously, performance expectations were classified into two main groups, namely low and high(Ciampoli et al., 2011). The former was related to safety

and integrity of the structure, whereas the latter was corresponded to serviceability requirements(Augusti et al., n.d.). However, other classifications can be found in the literature. For instance, FEMA(*FEMA Hazus-MH MR4. Multi-Hazard Loss Estimation Methodology: Earthquake Model, HAZUS-MH MR4: Technical Manual. Washington DC: Federal Emergency Management Agency*, 2003) introduced four performance objectives, namely operational, immediate occupancy, life safety, and collapse prevention. In this study, three performance expectations are defined in the PBFRE for structural systems subjected to freezing rain events (see Table 3.1).

Table 3.1 Classification of performance expectations for the framework

Class	Description	Damage level
Operational	Continued operation at the expected performance.	None or negligible damage to non-structural part and the system is completely integrated.
Damaged	No severe threat but the functionality of the system is degraded and might be associated with some financial costs.	The most crucial elements for preserving the structural integrity are undamaged but there could be several damaged structural elements and the structural integrity is jeopardized.
Collapse	The system is not functional anymore and the structural distress can be visually recognized.	Significant damage to the most important elements and the structure is not safe anymore.

It should be noted that each class in Table 3.1 could have different levels depending on numerous factors, such as the structural system. For instance, “Damaged” class for a wind turbine which is placed at the vicinity of a residential area could have more sub-levels than a transmission tower system that is installed in mountainous terrain.

3.4 Theoretical formulation

In the realm of performance-based engineering, the structural risk corresponding to a specific performance level within a predefined time span can be estimated by probability of exceedance for a specified value (s) of decision variable (s). Theoretically, the risk estimation problem can be formulation as

$$G(DV) = \int\int\int\int\int G(DV|DM).f(DM|EDP).f(EDP|IM,IP,SP).f(IP|IM,SP) \\ .f(IM).f(SP).dDM.dEDP.dIP.dSP.dIM \quad (3.7)$$

where $G(.)$ = complementary cumulative distribution function, DV = decision variable, $G(.|.)$ = conditional complementary cumulative distribution function, DM = damage measure, $f(.)$ = probability density function, DM = damage measure, EDP = engineering demand parameter, $f(.|.)$ = conditional probability density function, IM = intensity measure(s), IP = interaction parameter(s), and SP = structural parameter(s). Finding an accurate solution for Eq. (3.7) is not an easy task and it can be solved in alternative ways (e.g., analytical solutions (Jalayer & Cornell, 2004) and stochastic techniques(Porter et al., 2001)). Broadly speaking, Monte-Carlo Sampling and its deviations are used for solving Eq. (3.7); however, they typically pose an intensive computational cost to the problem. In some cases, they cannot provide an accurate solution due to several problems, such as high dimensionality, complexity of the problem, or need for too many samples (e.g., > 1e9 samples). To avoid the complexity, it is assumed that structural parameters and intensity measures are assumed to be uncorrelated, and their effects propagate through interaction parameters. For example, ice accumulation, as a one of hazards during freezing rain events, changes the shape of conductor. The structural parameter and

intensity measures in Eq. (3.7) will be affected by this change and this interaction is reflected in interaction parameters (drag and lift coefficients). Similarly, once the storm has settled down (i.e., shedding or melting process), change in conductor's shape will be shown as change in interaction parameters not structural parameters or intensity measures.

3.5 Proposed framework – structural scale

According to the Equation (3.7), a risk problem can be decomposed into seven modules, namely hazard analysis, structural characterization, interaction analysis, structural analysis, damage analysis, loss analysis, and decision making. Figure 3.3 The proposed performance-based framework for freezing rain events depicts the involved modules in the proposed framework.

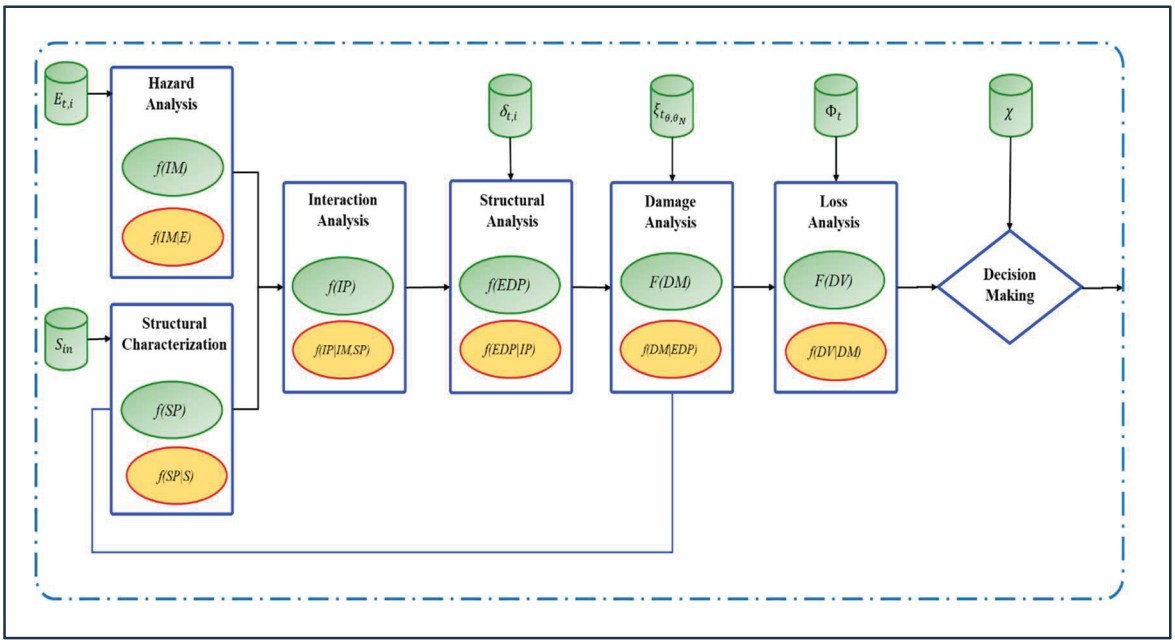

Figure 3.3 The proposed performance-based framework for freezing rain events

The challenging key which is disregarded in the literature is how the performance-based engineering frameworks can be applied for real-time prediction of an even-induced risk. Therefore, several cylinders, which indicate data from external resources, are added to the

framework. In Figure 3.3, $E_{t,i}$ = measured/estimated environmental parameters at time t or extreme values of environmental parameters within a specified span time, S_{in} = structural conditions (intact or aged), $\delta_{t,i}$ = experts recommendations or documentations in order to make the structural analysis more reliable, accurate and less computationally demanding, $\xi_{t_{\theta,\ \theta_N}}$ = real-time damage factors, Φ_t = real-time/anticipated financial cost of damage, and χ = experts comments/decision(s). It should be noted that the Performance-Based Freezing Rain Engineering (PBFRE) framework can be used for making the design of structural systems more robust and optimizing maintenance plan. The detailed description of each involved module in the PBFRE will be covered in the following.

3.5.1 Hazard analysis

The vector of Intensity Measures (IM)s is identified and characterized in this module to account for the associated uncertainties in freezing rain hazards. Eq. (3.8) expresses the vector of intensity measures for a freezing rain event (multi-hazards event).

$$IM = [IM_1, IM_2, \dots, IM_n] \tag{3.8}$$

where, n = the total number of involved intensity measures in freezing rain events (e.g., wind actions, freezing precipitation, and rainfall), IM_i = the vector of intensity measure for the i^{th} hazard that comprised of a vector of m×1 hazard parameters ($[H]_i^m$). Selection of these parameters are exclusively depended on the involved hazard and employed model for describing the hazard. For instance, the runoff will be treated as deterministic parameter if the recommended model by CSA 22.3 (i.e., Chaîné and Castonguay model) is employed. The concerning point is to avoid unrealistic estimation of the freezing rain event and fully describe the hazards and the ways in which they interact. Unnikrishnan and Barbato (Unnikrishnan & Barbato, 2017) classified the interaction between hazards them into three categories, namely independent, interacting and hazard chains. The first is based on limited number of marginal distribution function of each intensity measure (aka primary distribution model); the second is

based on a comprehensive set of intensity measures, each characterized by its respective marginal probability distributions (aka multiple distribution models); the latter is based on the suitable joint distribution function (e.g., Copula functions(Meng et al., 2024; Yang et al., 2020) or kernel density functions(Kong et al., 2020)). The proposed framework is flexible enough to readily implement all these interactions and even their combinations.

3.5.2 Structural characterization

The structural characterization module offers a stochastic description of structural parameters vector. These components determine the geometric and/or mechanical properties of the structure, which in turn define its response to both environmental and third-party loads. Eq. (3.9) expresses the vector of structural parameters subjected to freezing rain.

$$SP = [SP_1, SP_2, \dots, SP_n] \tag{3.9}$$

It should be noted that SP_i in Eq. (3.9) could represent the fundamental properties of a part of the system. For instance, a tower-line transmission system consists of several components, such as towers, insulators, conductors and earth wires. Each of these elements could have different SP values (i.e., a vector of s_i components). Moreover, depending on the type of structural system, which is assessed, there might need to consider other parameters. For example, the nominal voltage might be an important factor for cables as it not only accelerates the melting process but also causes elongation of the cables. Another example could be the number of spacers and their corresponding degree of freedom since they can dictate the torsional behavior of iced lines. In other words, solidification of supercooled drops and forming an iced coat demands the torsion of the cable. If the line is restricted, the ice deposit will fall due to its weight or wind effect that might ultimately lead to conductor jumping, collapsing the line, and power outage. Apart from these parameters, other parameters can also be found in the literature, such as robustness, connectivity, redundancy (Huang et al., 2001; Koh & See, 1994).

3.5.3 Interaction analysis

Interaction parameters (IP) define the dynamics between a structure and its environment, impacting how the structure responds and performs (see Eq. (3.10)). They also determine how environmental forces are distributed and intensified due to these interactions. For instance, aeolian vibrations are caused by wind pressure fluctuations on conductor surfaces due to vortex shedding and their corresponding frequencies of oscillations vary in the range of 3 to 150Hz with maximum amplitude of conductor's diameter. During freezing rain event, the ice deposit can exacerbate aeolian vibrations by locking conductor strands together, reducing internal damping due to strand slippage, and increasing conductor tension, which further decreases self-damping. Another example could be galloping movements which initiates by small perturbations and if wind blows in a specific angle of attack can onset a galloping oscillations, characterized by large amplitude (up to 15m) and low frequencies (Van Dyke et al., 2008b). To obtain the probability distribution of interaction parameters vector, it is essential to consider both intensity measures and structural parameters (i.e. $P(IP_i|IM_i, SP_i)$). In other words, the effect of intensity measures and structural parameters must be propagated to the interaction parameters. For instance, drag and lift coefficients in power-line transmission systems are dependent on several parameters, including the shape of iced structure. If the rate of precipitation or wind speed changes, this impacts the accumulation and the wind-induced force to the iced surface, consequently.

$$IP = [IP_1, IP_2, \dots, IP_n] \tag{3.10}$$

3.5.4 Structural analysis

The structural analysis module presents a probabilistic description of an appropriate engineering demand parameters vector, representing the essential aspects of structural response for damage and performance evaluation (see Eq. (3.11)). Examples of engineering demand parameters include force, moment, and stress state in structural and non-structural elements,

as well as response quantities like deflections, velocities, and accelerations at selected points, and structural deformation indices. It should be noted that structural analysis module typically requires a detailed model (e.g., finite element model) or field measurement methodologies or other alternatives (e.g., machine learning-based procedures(Thai, 2022)) to determine engineering demand parameters.

$$EDP = [EDP_1, EDP_2, \dots, EDP_n] \tag{3.11}$$

3.5.5 Damage analysis

The damage analysis module presents a probabilistic description of damage measures conditioned to the obtained engineering demand parameter values. The term "damage" in the module refers to any potential loss to the structural components or non-structural ones caused by the involved hazards during a freezing rain event. It is crucial to select a limit state function to develop to represent the severity of damage in terms of fragility curves (e.g., (Seyedeh Nasim Rezaei, 2016)). Limit state function is a mathematical expression or model used to evaluate whether a structure or component meets specific performance criteria under given loads and conditions. The limit state function is central to the concept of limit state design, which ensures that structures perform adequately throughout their service life. A limit state function *g(x)* is typically formulated as:

$$g(X) = R(X) - L(X) \tag{3.12}$$

where, $R(X)$ = the resistance or capacity of the structure (aka engineering capacity parameters), $L(X)$ = the applied load or demand on the structure (i.e., engineering demand parameters). The structure is considered to be in a safe state if $g(X) > 0$ (resistance exceeds load) and in a failure state if $g(X) \leq 0$ (load exceeds resistance). Let's define $U(X)$ as the structural status (see Figure 3.4); if $u(X) = 1$, it indicates the structural safety and if $u(X) = 0$ it implies the structural failure. Based on the total probability theorem, the total number of experiments

where the system was safe over the total number of experiments can represent the probability of failure of the structural system ($P(f) = {}^{n_{failed}}/_{N_{total}}$). As a result, this module could be the most computationally demanding part in the framework. Recently, machine learning-based alternatives have gained more reputation and have been successfully employed for development of fragility curves and estimation of damage measure values.

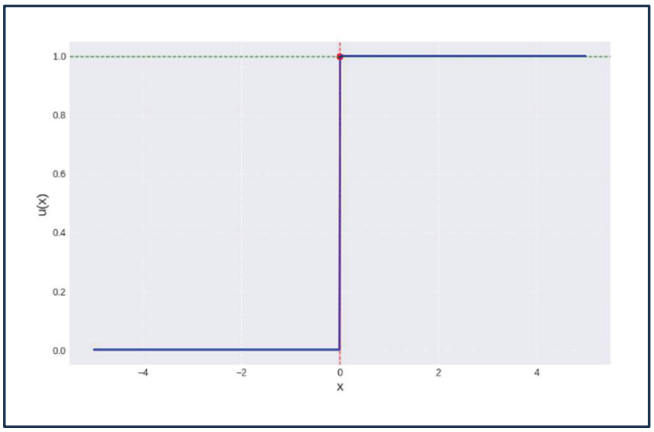

Figure 3.4 Unit function

3.5.6 Loss analysis

The module presents the total structural risk in terms of decision variables using the complementary cumulative distribution function. All ice-induced costs can be estimated in this module, such as retrofitting, injuries and human death, social service losses, factories production loss, among others. The obtained results can be further employed for decision-making on optimization of structural design shape, material or the configuration; adjustment of maintenance plan; devising an appropriate anti-icing or de-icing measures. Conventionally, structural risk is expressed in terms of different decision variables (monetary), such as repair costs due to the damage, down time, percentage of insured values, etc. (Barbato et al., 2013). However, if there is a practical model, some specific losses (e.g., ethical losses) can be expressed in terms of other indices (e.g., psychological decision variables) rather than monetary ones.

3.6 Proposed framework – spatial scale

Application of the PBFRE framework for spatial scale is challenging due to the inessive computational cost required for solving Eq. (3.7). Utilizing numerical approaches (e.g., Monte Carlo simulation and its deviations) for solving the equation needs integration of each module and might even require numerous samples to reach a reliable result. In addition, the structural analysis module is based on Finite Element (FE) with a fine mesh significantly increases the computational cost. Alternatively, data-driven techniques (e.g., support vector machine) and complementary methods (e.g., deep autoencoder, deep learning-based time series forecasting) can be employed. However, it should be noted that freezing rain events are typically rare and occur over short periods that make devising an early warning system intractable. For instance, Snaiki and Shabani(Snaiki & Shabani, 2023) employed a deep learning neural network for quick prediction of the worst ice storm-induced risks in Arkansas. In the literature few interesting simplified solutions can be found (e.g., (Snaiki & Shabani, 2023)) that used deep learning methods for identification of high risk areas in spatial scale and solve Eq. (3.7) for structural scale. In is of great importance to note that although applying the framework at spatial scales could potentially pose more complexity and uncertainties, either aleatoric or epistemic, to the risk problem. The PBFR framework could address uncertainties arising from incomplete data or unknown variables by integrating probabilistic modeling and advanced machine learning techniques. Probabilistic approaches, such as Bayesian inference, facilitate the continuous updating of risk estimations by incorporating new data, thereby effectively accounting for epistemic uncertainties. Machine learning models complement this by identifying latent patterns, imputing missing data, and enhancing predictive accuracy in the presence of incomplete information. Furthermore, stochastic simulations, such as Monte Carlo methods, enable robust quantification of variability and uncertainty, ensuring reliable risk predictions under complex and dynamic conditions.

3.7 Application

The proposed framework's application is illustrated through the risk assessment of a tower-line transmission network (see Figure 3.5) exposed to freezing rain events. The objective of the application section is to highlight the flexibility and effectiveness of the PBFRE framework at both design and maintenance (i.e., structural and spatial scale) for real-time freezing rain-induced risk forecasting in cold regions. Therefore, the application step is carried out for two applications, namely maintenance planning and design. In the maintenance planning part, the freezing rain-induced for a tower transmission tower-line system (see Figure 3.5) at two scales (i.e., structural and spatial) and PBFRE framework leverages the capabilities of an advanced data-driven model to address the associated computational cost for solving the risk problem. For design part, the application is demonstrated only at spatial scale. Extreme freezing rain map based on the historical spatiotemporal climatological observations across the US is developed by using a novel approach and IoT principles are utilized to address the issues of real-time prediction of freezing rain risks for vulnerable structural systems.

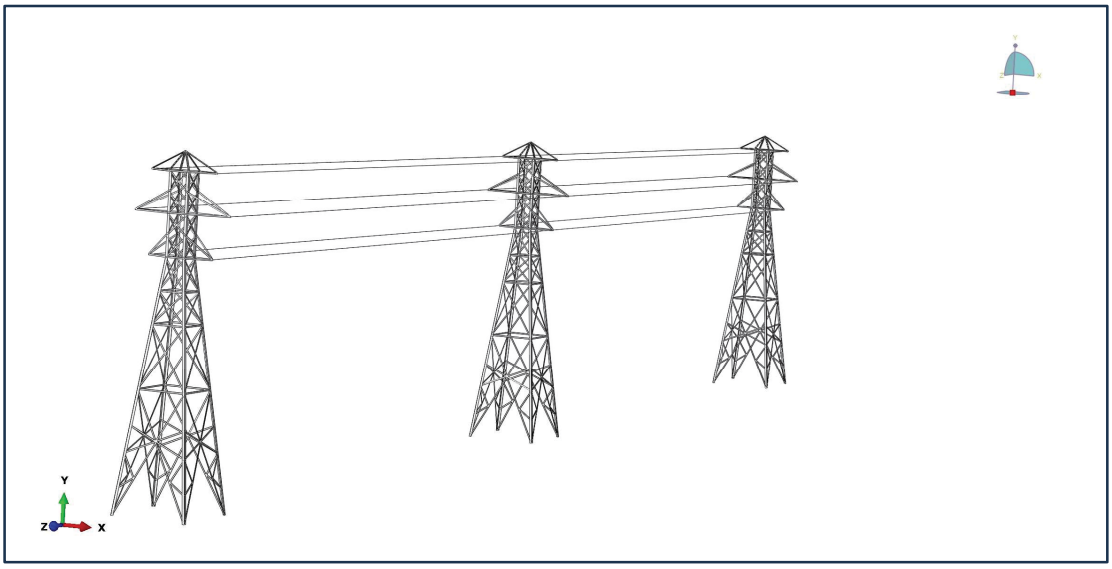

Figure 3.5 Finite Element model of tower-line transmission network

3.7.1 Maintenance

3.7.1.1 Structural scale

The main objective of PBFRE framework at structural scale is to solve the risk problem (i.e., Eq. (3.7)) for a specific structural system prone to freezing rain event. As a result, the systematic procedure for solving the aforementioned equation must be carried out. As a result, primarily the performance expectations need to be defined and then each involved module in the problem can be discussed. It is of great importance to note that engineering demand parameters are assumed to be equivalent to damage measures (i.e., $EDP = DM$) and loss analysis disregarded due to lack of accurate financial data.

3.7.1.2 Performance expectations

As it was stated in section 1.1.1.3, three performance expectations, namely operational, damaged, and collapse, are defined within the PBFRE framework. Since wind actions-induced load on iced conductors can be considered as a cyclic load, fatigue models can be employed. If any permanent deflection in conductors are assumed to be unacceptable, then according to Palmgren-Miner rule the accumulated damage (D_{tot}) can be obtained using(Nussen & Van Delft, 2003; M. M. Shabani et al., 2017):

$$D_{tot} = \sum_{i=1} \frac{n_i}{N_i} \tag{3.13}$$

Where, n_i = the number of cycles during ith experiment and N_i = the number of cycles that could lead to structural failure due to load, L_i, with constant amplitude of A_i. Therefore, fatigue life of the conductor (T_{fat}) in presence of no permanent deflection can be formulated as:

$$T_{fat} = {}^{\eta}/_{D_{tot}} \tag{3.14}$$

Where, η = a constant that should be determined for each material. Based on the Eqs. (3.14) and (3.15), three limit state functions can be derived:

$$g_1 = 1 - D_{tot} \tag{3.15}$$

$$g_2 = T_0 - T_{fat} \tag{3.16}$$

$$g_3 = 1 - {T_{fat}}/{T_0} \tag{3.17}$$

Where, T_0 = predefined fatigue life for the conductor (e.g., 20 year or 40 years). Accordingly, the limit states for quantification of the freezing rain-induced risk have been selected and listed in Table 3.2. It should be noted that the idea of unit function will be changed by this definition since g values larger than 1 imply safety and g values equal to zero indicate structural failure.

Table 3.2 Risk levels

Risk class	Risk level	Limit state value (g_1&g_3)
Operational	Slight	≥ 0.5
Damaged	Moderate	> 0.15 & < 0.5
Collapse	Extensive	≤ 0.15

3.7.1.3 Hazard analysis

As previously discussed in section 1.1.2, two hazards are the most seen during freezing rain events: ice accumulation and wind actions. Jones et. al(Jones et al., n.d.) stated that maximum 3-seconds gust wind speed and total ice accumulation within the storm are the most dominant hazards. To highlight the performance of the PBFRE framework in estimation of freezing rain-induced risk over a large area, a real freezing rain event which occurred between the 4th and 5th of December 2002 in Arkansas has been selected as a case study. The climatological

inoformation is retrieved from Automated Surface Observing System (ASOS) that is available online that provides weather information for a location – often, airports – at regular intervals. Reporting intervals are generally hourly, but sub-hourly reports are created when changing weather conditions are detected by automated sensors or a supplemental human observer, if available. A typical ASOS station includes sensors to measure pressure, wind, temperature, dew point, visibility, and cloud height. Generally, temperature is reported in Fahrenheit (°F), wind speed in knot, and precipitation in inch. Quality control is conventionally done using control software to correct possible errors and those records which require manual correction will be flagged. Observations (hourly) which are reported with freezing rain indices ("FR" and "FZRA") and freezing drizzle ("FZDZ") are extracted from reports. Observations without precipitation records (missed) are excluded from the dataset. The maximum value of average of measured wind value within radius of $10km$ or $0.1^{m}/_{sec}$ ($\approx 0.195\ knot$) is used for observations where wind value is missed. Wind values were adjusted using power law by assuming that all measurements were done in airports to represent average hourly wind speed (see Eq. (3.18)).

$$V = V_0 \left(\frac{z_1}{z_0}\right)^{0.1428} \tag{3.18}$$

Where V_0 = wind speed measured at height z_0, z_1 = 10 m, and z_0 = reference height. The mean wind speed values were multiplied by a gust wind speed coefficient (1.36) to obtain 3-seconds wind speed (Arriaga, 2020). Ice thickness was estimated using CRREL model(Finstad et al., 2003) where the ice thickness in cylindrical shape, R_{eq}, is formulated as:

$$\Delta R = \frac{1}{\rho_{ice}\pi} \sum_{t=1}^{N} \sqrt{(P_t \rho_t)^2 + (3.6 V_t W_t)^2} \tag{3.19}$$

Where, W_t = the liquid water content that can be estimated using Best model(Best, 1950).

$$W_t = 0.067 * P^{0.846} \tag{3.20}$$

Although the Marshal and Palmer model(Marshall & Palmer, 1948) is also practical, Jones(Jones, 1996a) recommends the Best model (i.e., Eq. (20)). It should be noted that the diameter is assumed to be one inch (i.e., 25.4 mm). Typically, ice deposit is expressed in terms of ice eccentricity (i.e., $e = \frac{t}{d}$)as it is depicted in Figure 3.6 (Poots & Skelton, 1995). In this study, the semi-ellipse profile proposed by Poots & Skelton(Poots & Skelton, 1995) are employed. Although more accurate profiles (e.g., Fu et. al (P. Fu et al., 2006)) can be found in the literature, semi-ellipse is selected due to its simplicity.

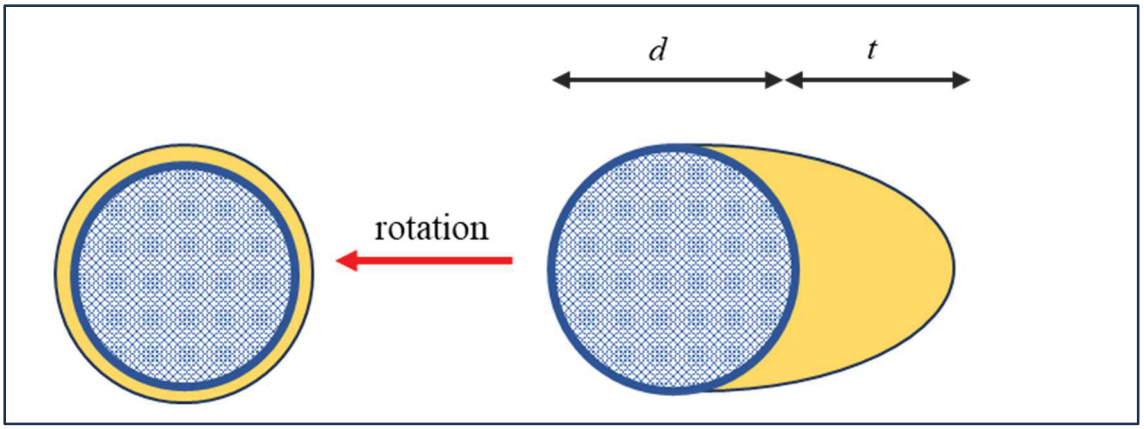

Figure 3.6 Simplified ice profile

Let's assume that there is no sublimation, melting (run-off) and wind speed remains constant throughout the rotation. Therefore, the equivalent radius of accumulated ice in radial shape (ΔR) can be ideally obtained using mass continuity equation and expressed as:

$$\Delta R = \frac{d}{2}\left(\sqrt{1+\frac{t}{d}}-1\right) = \frac{d}{2}\left(\sqrt{1+e}-1\right) \tag{3.21}$$

Similarly, the ice deposit in semi-elliptical shape can be formulated as

$$t = 4\Delta R\left(1+\frac{\Delta R}{d}\right) \tag{3.22}$$

For structural scale, retrieved data from stations (RUSSELLVILLE and FORT SMOTH MUNI) are utilized. As a result, there are limited number of precipitation and wind speed observations during the storm). Although this limited number of observations may not be enough for estimation of risk accurately, it is deemed sufficient to use them to showcase the application of PBFRE framework and its effectiveness. Generalized Pareto and Weibull distribution are chosen for representing ice accumulation and 3-seconds gust wind speed, respectively(Jones et al., n.d.). The parameters are acquired through fitting distribution to historical site-specific climatological observations. Although advanced approaches, such as copula functions (Yang et al., 2020) can be employed for including the joint effect of wind speed and ice accumulation, both hazards are assumed to be statistically independent (see Eq. (3.23)).

$$P(A \cap B) = P(A) * P(B) \tag{3.23}$$

3.7.1.4 Structural characterization

The structural system is assumed to be flawless and intact. The aging effect is excluded from the current study for the sake of simplification. Moreover, the effect of Dynamic Line Rating (DLR), spacer, and anti-icing are ignored. The conductor is assumed to be Aluminum conductor steel-reinforced cable (ACSR) and transmission tower is made of galvanized steel. The towers are completely fixed to the ground, but the conductors can rotate. The diameter is one inch, and conductors are homogeneous. At the beginning of the storm, the system is assumed to be fully functional and completely integrated. The considered structural parameter is: Young modules that follows Log-normal distribution with the mean value equals to the nominal value and coefficient of variation of 0.03(X. Fu et al., 2020). It should be noted that some studies consider conductor's diameter as part of structural parameters (e.g., (Snaiki & Shabani, 2023)) that could be inaccurate in some cases because of the effect of diameter on nucleation and accumulation rate. In addition, the interaction between conductor's diameter

and ice accumulation has to be included. That requires profound understanding of atmospheric icing and solving the heat balance equation, and it is beyond the scope of current study.

3.7.1.5 Interaction analysis

This study employs a simplified formula, which is proposed by CSA-22.3, to capture interaction analysis through wind pressure load (see Eq. (3.24)).

$$A = q_0 . C_d . G_L . G_c . d_{iced} . L \tag{3.24}$$

where q_0 = dynamic wind pressure, C_d= drag coefficient, G_L = span factor, G_C = combined wind factor, d_{iced} = the diameter of iced conductor with ice coat, and L = the span length. Determining wind-induced forces on irregular surfaces, like Figure 3.6, analytically or numerically is complex. Generally, icing wind tunnel experiments or advanced computational fluid dynamic models are utilized to obtain drag coefficient. Several studies can be found in the literature (e.g., (Brown et al., 2014))where investigated the most important parameters on drag coefficient of an iced conductor. Essentially, three parameters dictate the variation of drag coefficients: 1. Wind speed, 2. Angle of attack, and 3. Shape of iced body or simply the eccentricity's shape and dimension. Alternatively, a deep learning model is trained based on the icing wind tunnel test results obtained by Rossi et. al(Rossi et al., 2020). The network's architecture is expressed in Table 3.3.

Table 3.3 Deep learning architecture for prediction of C_d

Param	Value
Inputs size	3
Output size	1
Hidden layer	2
Number of neurons	64-36
Optimizer	Stochastic gradient decent
Epoch	400
Training split ratio	70%
Scaler	MinMax
Early stopping	patience =10 tol=1e-5

The obtained metrics for evaluating the network performance are:

Table 3.4 Metrics obtained for measuring network's performance

Dataset	Metrics	Value
Training	MSE	1.83e-3
	R2 score	97.6%
Testing	MSE	2.3e-3
	R2 score	89.3%

It can be clearly from Table 3.4 that the model is trained properly and has an acceptable performance.

3.7.1.6 Structural analysis & damage analysis

The structural condition in this study was obtained through a FE model that was developed in ABAQUS/CAE 6-14 (see Figure 3.7). The conductors were modelled as wire (cylindrical) and the loads (ice layer weight and wind load) were applied as line load. Structural parameters were considered as deformable 3D elements.

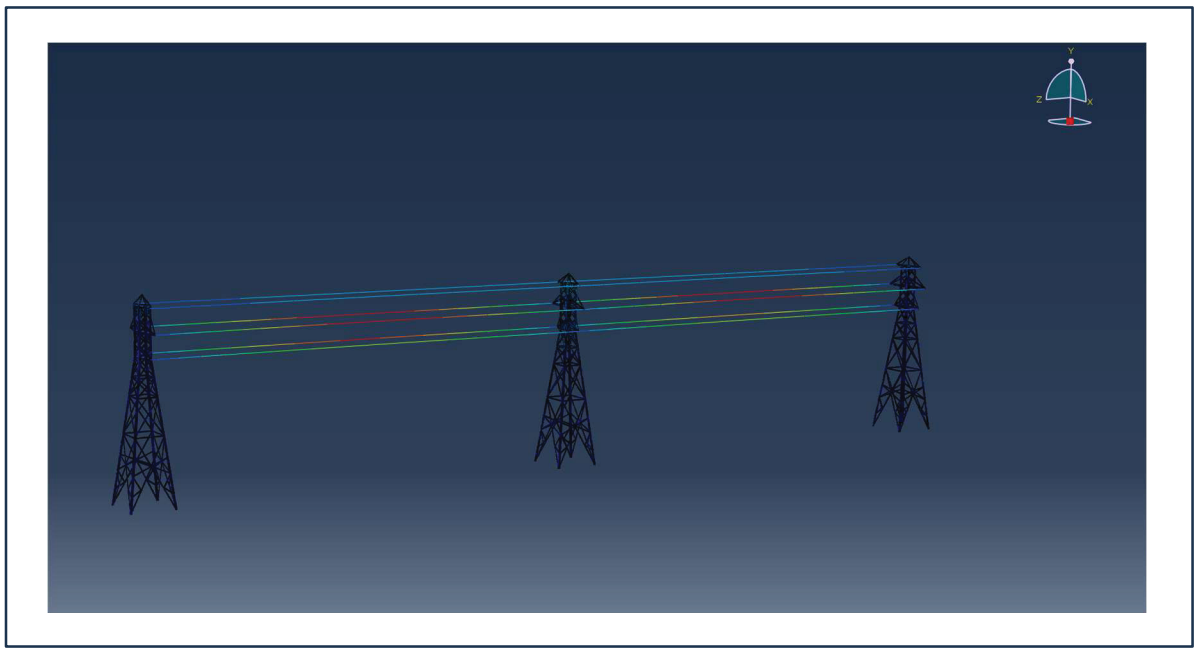

Figure 3.7 The employed FE model for tower-line transmission system

The model was executed on processor unit with the following specifications: an Intel Core i7-12700H processor and 16 GB of DDR5 RAM. To obtain the damage measures, it is necessary to use a limit state function; the Eq. (15) was employed in this study. To solve Eq. (3.7), importance sampling based on First-Order Second-Moment (FOSM) was utilized. The stopping criteria was selected to be either reaching to the maximum number of samplings

(1,000,000 samples) or coefficient of variation of obtained probabilities be lower than 5%. By considering the fact that executing the model for each scenario was taken approximately 300 seconds, estimating the probabilities takes around several weeks. To address this issue, advanced numerical approaches or deep learning-based procedures can be used. Liu et. al(Liu et al., 2023) illustrated the effectiveness of Sparse Identification of Nonlinear Dynamics (SINDy) (Brunton et al., 2016) in the identification of the governing dynamic of iced bundle conductors. The galloping equation of the iced conductor can be formulated as an ordinary differential equation (see Eq. (3.25)).

$$\frac{d}{dt}X(t) = f(X(t)) \tag{3.25}$$

Where, $X(t)$ = the vector of system's state at time *t* and $f(X(t))$ = dynamic constraint of EOM. The sparse identification method enables the discovery of the sparsity structure in complex, unknown dynamical systems. This approach allows for the identification of a parsimonious model that includes only the essential nonlinear terms. In order to obtain function, $f(X(t))$, the system's state vector should be collected and derived to acquire two matrices ($X(t)$ and $\dot{X}(t)$) and determine the nonzero coefficients of the spare regression problem (see Eq. (3.26)).

$$X = \Theta(\dot{X}) * \Xi + \psi \tag{3.26}$$

Where, Θ = the candidate functions in the vector of N^{th} order polynomial, Ξ = the sparse expansion coefficients, ψ = the matrix of noise. Since the limit state functions are defined as a function of structural stress and structural stress can be obtained from structural strain if there is no permanent deformation, SINDy can identify the governing dynamic of iced conductors' oscillations to obtain structural displacement. Integration of the approach leads to addressing the issue of intensive computational cost for executing the FE model and contributes to immediate estimation of desired parameters. Using the defined limit states (Table 3.2), the potential risk of onset and development of galloping has been calculated using the Importance

Sampling technique based on FOSM estimation. The obtained results are presented in Table 3.5.

Table 3.5 Estimated potential galloping risk to the iced conductor

Station	Slight	Moderate	Extensive
RUSSELLVILLE	96.3%	3.5%	0.2%
FORT SMOTH MUNI	89.23%	8.97%	1.8%

As Table 3.5 indicates, the possibility of collapse in the second station is relatively higher that necessitate design and implementation of anti-icing techniques or prepare other considerations to mitigate the freezing rain-induced risk.

3.7.1.1 Spatial scale

In this section, the application of PBFRE for the spatial scale (maintenance) will be illustrated through galloping-induced risk for iced conductor throughout an extensive area. In order to demonstrate the excellent application of PBFRE framework in prediction of freezing rain threat to vulnerable systems, a real storm that occurred between 4th and 5th of December of 2002 in Arkansas is selected. Once the quality control was carried out, the total ice accumulation within period of one hour was estimated using CRERL model(Jones, 1998). Due to limited number of stations (16), a simple linear spatial interpolation technique is employed to improve the resolution of data within spatial scale. As the major aim of the current study is to demonstrate the effectiveness of PBFRE framework, simple spatial interpolation technique is utilized while advanced super resolution approaches can also be utilized. The interpolated ice eccentricity and gust wind speed maps are displayed in Figure 3.8.

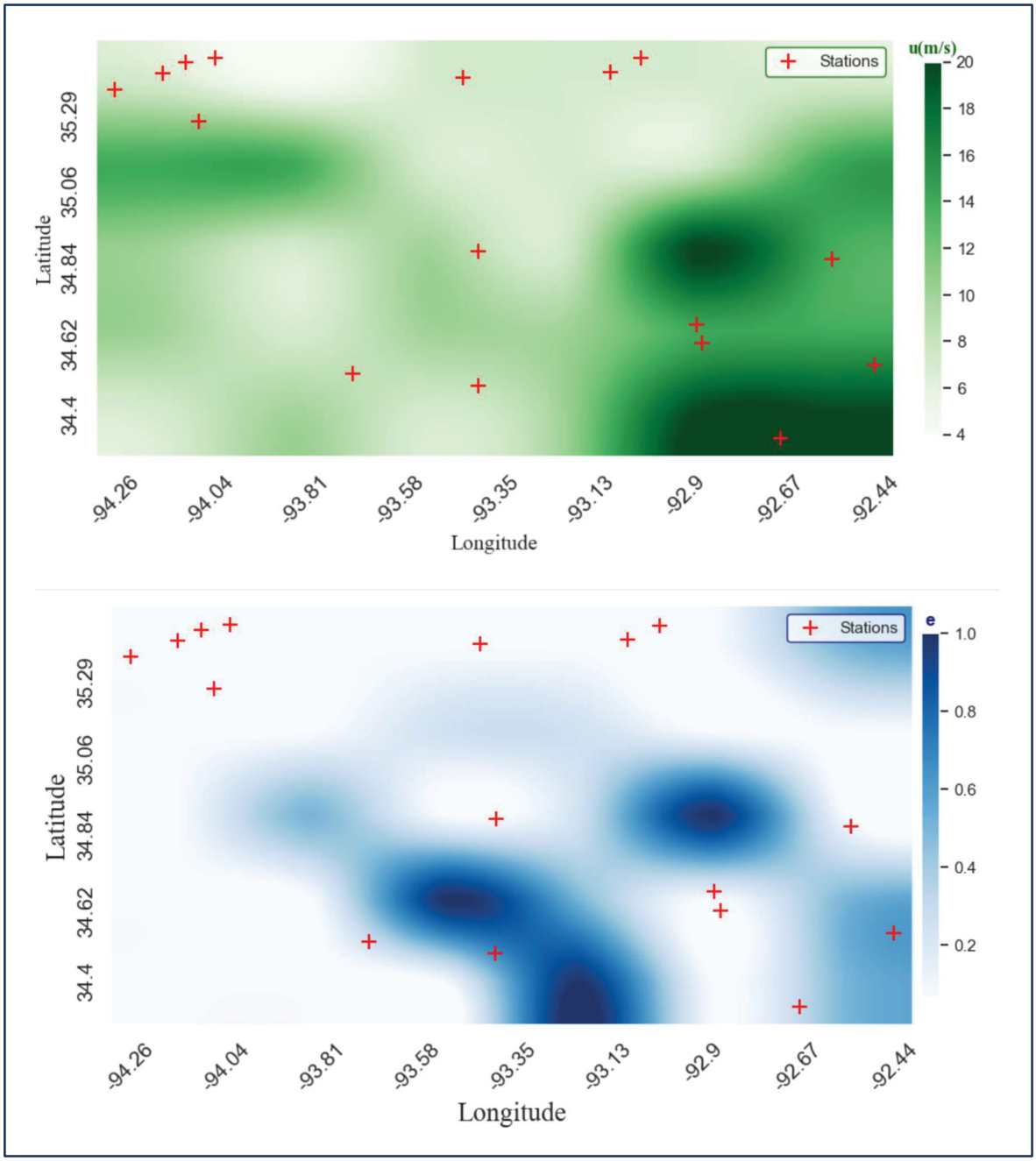

Figure 3.8 Map of gust wind speed (top) and ice eccentricity (bottom) for 4th and 5th of December 2002 storm in Arkansas

Similar to the structural scale, the fitted SINDy model will be fitted to retrieved data from stations (16 stations) to identify the dynamics of iced conductor more accurately. Similar to previous section, importance sampling based on FOSM estimation was utilized to solve Eq.

(7) for more than 180 interpolated points across domain and Eq. (3.15) was selected as the limit state function. It should be noted that the angle of attack was assumed to be $170°$ which implies the worst galloping condition(Rossi et al., 2020). This pessimist assumption was taken as the angle of attack is usually not reported at the selected ASOS stations. Similar solver based on the same termination trigger mechanism was employed for solving the Eq. (3.7). The structural status was evaluated and express in three performance expectations, namely operational, damaged, and collapse. The exploit the system's potential as much as possible, a batch with 100 samples was defined to reduce the processing time. Therefore, 100 samples were generated during each iteration for solving the Eq. (3.7), resulting in a reduction of the processing time by more than 70%. Figure 3.9 depicts the generated freezing rain-induced risks at different levels. It is of great importance to note that in the slight level, the limit state function is adjusted to ignore $g \geq 1$.

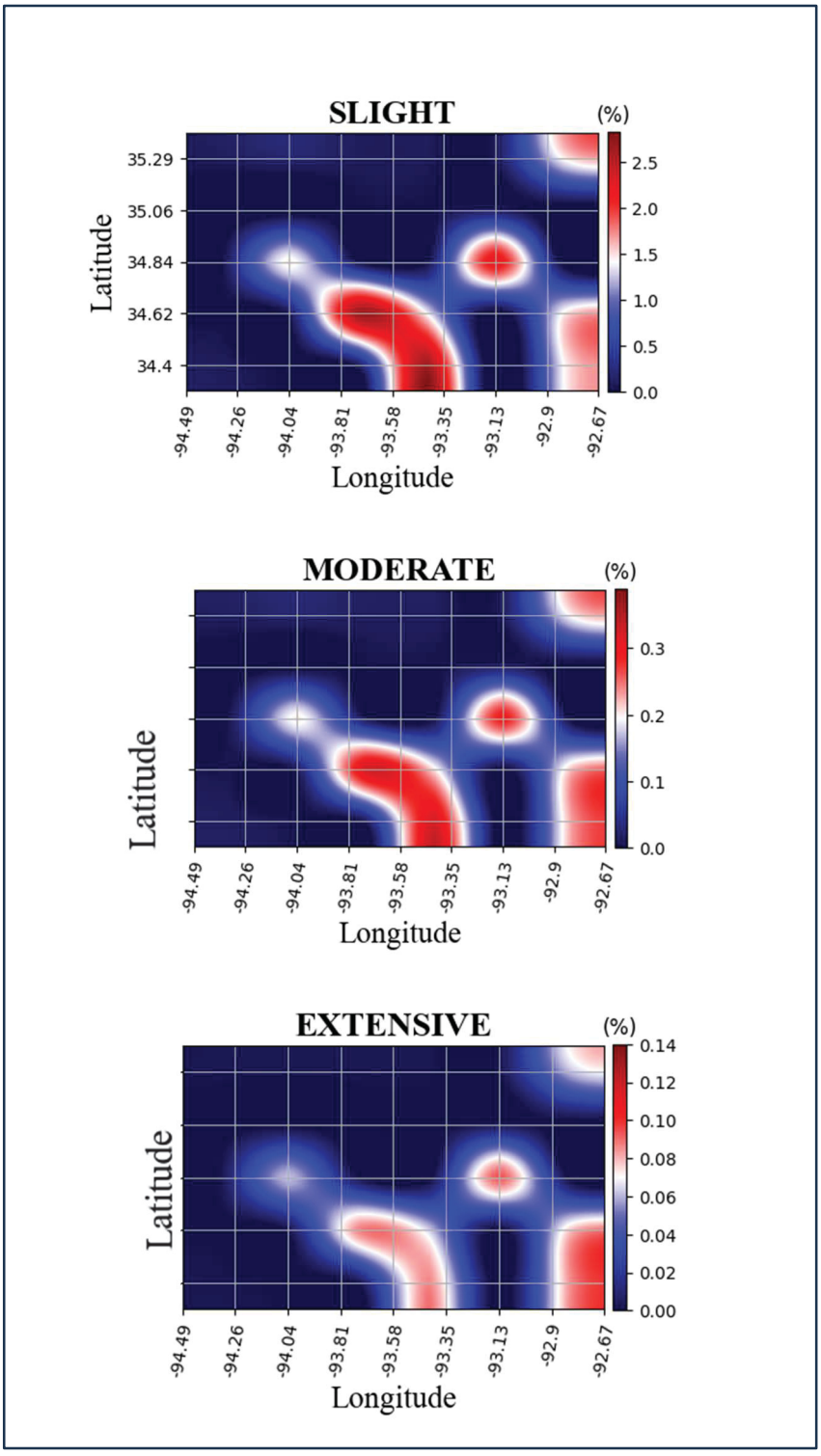

Figure 3.9 Galloping risk levels at spatial scale with angle of attack = 170°

It is crystal clear in Figure 3.9 that the red areas might experience high galloping-risk levels. Hence, anti-icing techniques, such as weakening the adhesion strength of ice, adding chemicals to prevent the nucleation, and novel approaches to restrict the accumulation on the conductor must be designed for alleviating the ice accumulation impact on onset of the conductor's instabilities in those areas. It is of great importance to note that a different strategy is employed in developing Figure 3.9, it shows the most severe risk level in the station. To exclude very small and negligible values, especially in extensive level, a threshold is defined.

3.7.1 Design

The second objective of the application part is to show the effectiveness of the PBFRE framework for design of structural system prone to extreme freezing rain events. Therefore, the following sections will elaborate development of the freezing rain-induced risk maps.

3.7.1.1 Hazard analysis and structural characterization

As previously discussed, two hazards are mostly reported during freezing rain events: (1) ice accumulation and (2) wind actions. Canadian Standard Association (CSA) sets up three reliability levels for design of transmission systems prone to freezing rain events as the minimum acceptable return period: (1) level I: 50 years, (2) level II: 150 years, and (3) level III: 500 years. Selection of suitable target return period must be made based on the voltage of the line. Herein, it is assumed that 50 years is suitable for the line. CSA-22.3 proposes two combinations for design of transmission lines in cold regions:

1. C1: T-years return period ice accumulation with the low probability + average annual 3-seconds gust wind speed with high probability.
2. C2: T-years return period ice accumulation with the high probability + average annual 3-seconds gust wind speed with high probability.

Jones et. al (Jones et al., n.d.) characterizes a freezing rain event with modest wind speed. Since wind speed is typically less than 15 $^{m}/_{sec}$ during freezing rain events(Arriaga, 2020), it can be concluded that C1 is mostly the worst scenario. Although it may reduce the complexity of the icing problem and its associated aerodynamic aspects, it does not necessarily guarantee the integrity of transmission systems. Therefore, it is crucial to develop a more accurate extreme freezing rain map. In the following subsection a novel approach for developing extreme freezing rain maps is provided.

3.7.1.2 Data retrieval

The historical spatiotemporal climatological observations are retrieved from ASOS, which is available online. Once the Extract, Transform, and Load (ETL) process is completed, complementary adjustments, including unit conversion and wind height base measurement, are carried out. The extraction of freezing rain data is then conducted based on the Meteorological Aerodrome Report (METAR); different indices are included, such as “FR”, “FRZA”, “FZ”, and “FZDZ.” The data is collected from more than 900 stations (see Figure 3.10), covering the period from 1975 to 2020. As ice accumulation is not reported for some periods, it is imperative to estimate total ice accretion within period of one hour. Although, it may seem more accurate to employ the period of freezing rain storms as the base for studying, one hour is preferred since typically the initiation and dissipation points are not essentially known and reported. Prediction of ice accretion is basically associated with several challenges and empirical/experimental models are generally preferred. In literature, several attempts can be found for improving prediction of ice accretion in cold regions (e.g., (Diem, 1956; Jones, 1996a, 1998; Makkonen, 1998, 2000; Rudzinski et al., 2005; Wright, 1999)), however, few studies (e.g., (Jones, 2023; Sheng et al., 2023)) can be found that investigate the effect of different models on mapping extreme maximum annual ice accretion. In addition, the CSA-based method for prediction of concurrent wind speed is impractical and cannot necessarily

guarantee the system's integrity. Therefore, it is of great importance to do an investigation and identify the best prediction model for the case study.

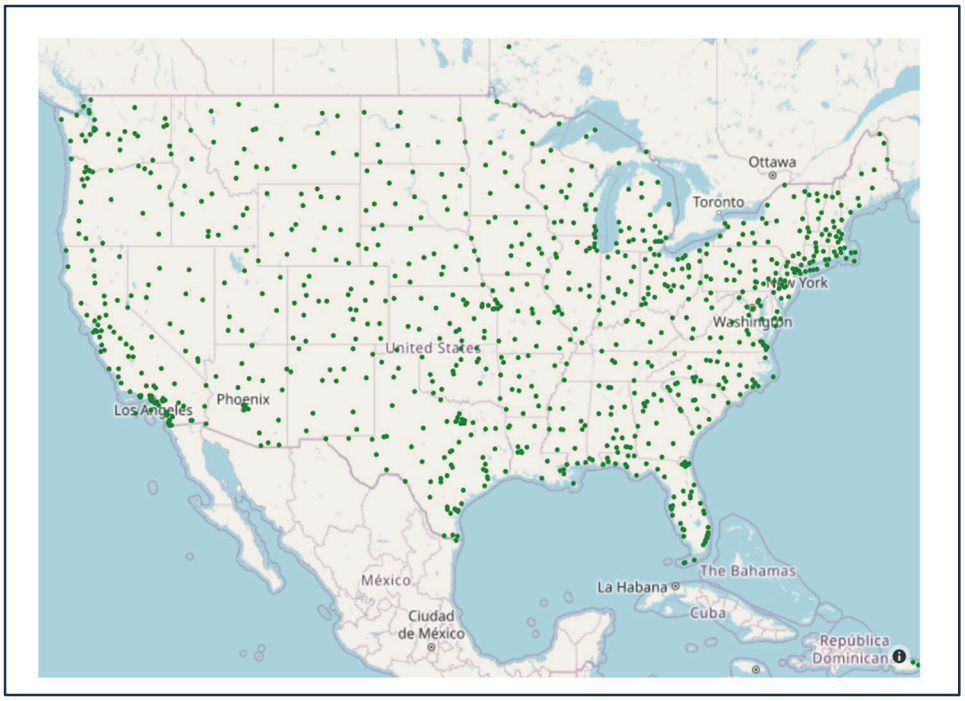

Figure 3.10 List of active stations in the US

3.7.1.3 Ice accretion prediction

To predict ice accretion, three mostly used models, namely Goodwin, Chaîné and Castonguay, and CRRREL are employed. Each model is developed based on different assumptions that are discussed. The type of ice in all cases is assumed to be "glaze ice" with density of 0.9 $^{gr}/_{cm^3}$. Although this pessimist assumption might lead to overestimation in some stations, it reduces the complexity of ice estimation problem since density of the ice layer is a function of wet bulb temperature and impact droplet velocity(Macklin, 1962). It should be noted that the conductor's diameter is assumed to be one inch and the ice layer characteristics are distributed homogeneously along the line. The Goodwin model is develop based on the assumption that all supercooled drops freeze on the impinged surface and neglects the effect of bouncing and

runoff. Based on the model, the change in diameter of a one-inch rod in cylindrical shape (ΔR [mm]) can be estimated using Eq. (3.28).

$$\Delta R = \frac{\rho_w H_g}{\rho_{ice}\pi}\sqrt{1+\left(\frac{V}{V_d}\right)^2} \tag{3.27}$$

$$V_d = \begin{cases} 8 * r_0 & r_0 < 0.6 \\ 201 * \sqrt{\frac{r_0}{1000}} & 0.6 \leq r_0 < 2 \end{cases} \tag{3.28}$$

$$r_0 = {}^{1.835}/_{4.1}\, P^{0.21} \tag{3.29}$$

Where, $\rho_w({}^{gr}/_{cm^3})$ = density of water, H_g (mm) = depth of liquid precipitation, V_d $({}^{m}/_{sec})$ = mean wind speed, r_0 (mm) = median raindrop size, and P $({}^{mm}/_{hr})$ = rate of precipitation. The second model which is recommended by Canadian Standards Association (CSA-22.3) is developed by Chaîné and Castonguay (Chainé & Castonguay, 1974) based on the assumption of freezing all impinged drops on the surface. Similarly, this model also ignores the effect of run-off and bouncing. In addition, the model neglects the fact that all drops cannot necessarily stick to the surface due to several factors, such as wind speed. Based on the Chaîné and Castonguay model, change in diameter of a one-inch rod can be estimated using Eq. (3.31).

$$\Delta R = \sqrt{\frac{RK}{2}\sqrt{T_v^2 + T_h^2} + R^2} - R \tag{3.30}$$

$$T_v = 4.4316V * \left(\frac{P}{25.4}\right)^{0.88} \tag{3.31}$$

Where, $T_h(mm) =$ total freezing precipitation during one hour interval that is equal to P. The model assumes that the iced conductor has an elliptical shape and K is a correction factor. An

empirical model for computing *K* based on ambient temperature and radius of rod can be found in Ref. (Stallabrass et al., 1967). The most challenging issue in Eq. (31) is the dependency of the model on the radius of conductor and estimation of correction factor. Jones(Jones, 2023) in a comprehensive study showed that this model overestimates ice accretion and may not be effective. The last model, CRREL(Jones, 1996a), is developed based on the assumption of collision efficiency is 100%. In other words, if a supercooled drop does not bounce and could stick to the impinged surface, it will freeze completely. Let's compare it with the Makkonen model (i.e., ISO-12493 model)(Makkonen, 2000) that is developed based on solving the heat balance equation and is quite accurate (see Eq. (3.32)).

$$\frac{dM}{dt} = \alpha_1 \alpha_2 \alpha_3 WVA \tag{3.32}$$

Where, M= the total mass of accreted ice within the period of Δt, α_1 = collision efficiency, α_2 = sticking efficiency, α_3 = accretion efficiency, and A = the cross section of the cable. For glaze ice, collision efficiency and sticking efficiency are equal to one (i.e., $\alpha_1 = \alpha_2 = 1.0$) and α_3 can be obtained by resolving the heat balance equation on the impinged surface(Makkonen, 2000). Let's define 100 combinations of hourly precipitation and 3-second gust wind speed and assume that there is no runoff, ice type is "glaze" with density of 0.9 $^{gr}/_{cm^3}$, $\alpha_1 = \alpha_2 = \alpha_3 = 1.0$, and wind speed is invariant during each Δt in one hour. Therefore, Eq. (3.32) can be rewritten in this form.

$$\Delta R = \frac{d}{2}(\sqrt{1 + WV} - 1) \tag{3.33}$$

To do a comparison, total of 100 combinations of inputs in both models (i.e., hourly precipitation and wind speed) are simulated using Monte Carlo method and total accreted ice is calculated using Eq. (33) and Eq. (21) by considering the simplified assumption. The obtained mean absolute error ($\frac{\sum_{t=1}^{N} |x_{1,t} - x_{2,t}|}{N}$) and r2 score ($1 - \frac{RSS}{TSS}$) are 9.372 (mm) and 90.6145%, respectively. These results indicate how much CRREL model is accurate and can

be applied for prediction of glaze ice accretion. Based on the aforementioned models, the hourly ice accretion is computed for each observation and the maximum value in each station is depicted in the following images.

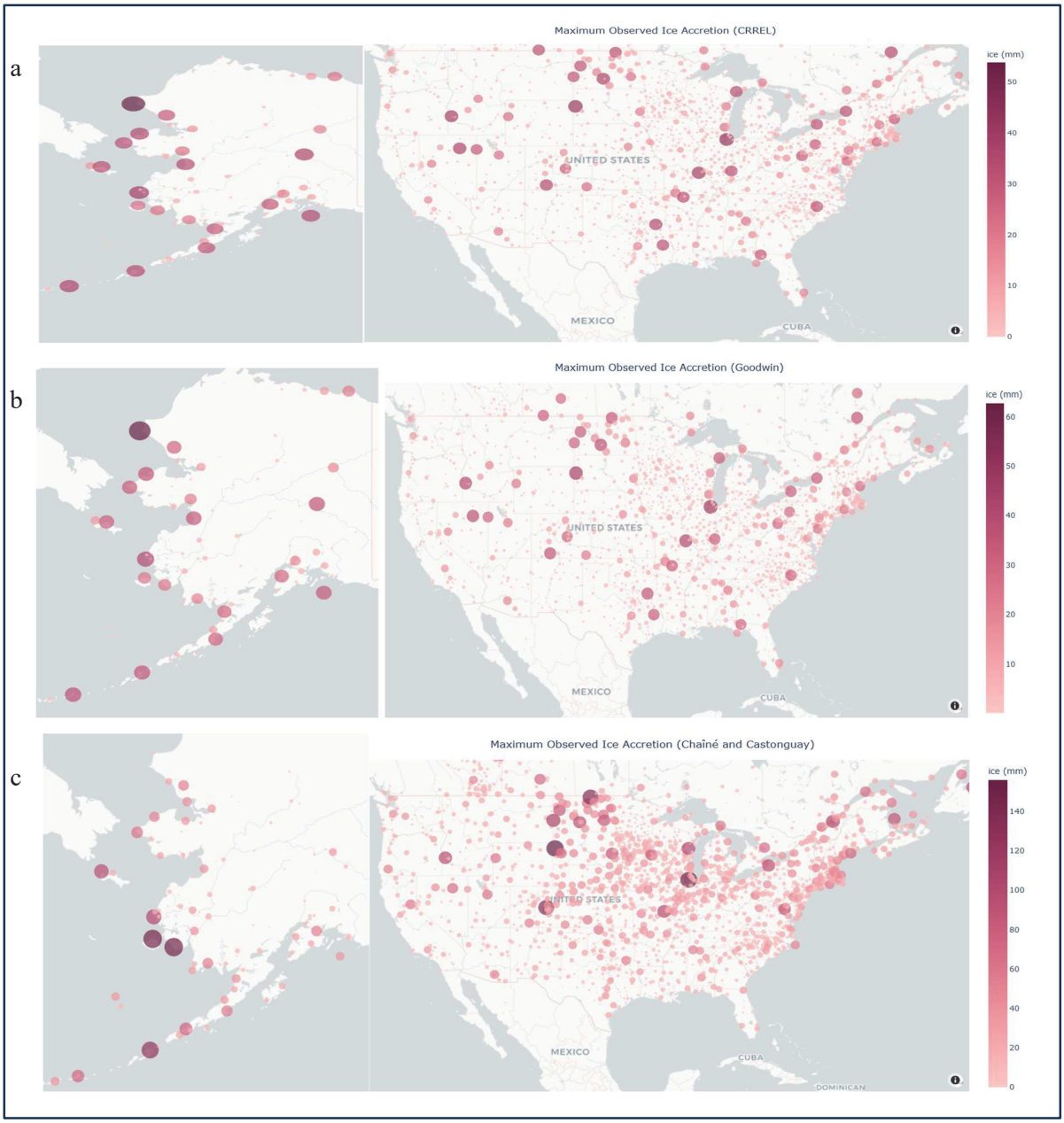

Figure 3.11 Maximum estimated ice accretion using three employed models: CRREL (a), Goodwin (b), and Chainé and Castonguay (c)

As Figure 3.11 shows, the estimations in Chainé and Castonguay model is comparably higher than the others; the maximum estimation in Figure 3.11.c is almost two times higher than the maximum prediction in Figure 3.11.a. To illustrate the difference among the employed models, mean absolute error and mean squared error ($\frac{\sum_{t=1}^{N}(x_{1,t}-x_{2,t})^2}{N}$) are calculated and listed in Table 3.6.

Table 3.6 Computed Metrics among for employed models

Comparison	mean squared error (mm^2)	mean absolute error (mm)
CRREL – Goodwin	0.08	0.06
CRREL - Chainé and Castonguay	267.25	9.72
Goodwin - Chainé and Castonguay	261.20	9.66

As Table 3.6 implies, Chainé and Castonguay overestimates the amount of ice accretion. It should be noted that Goodwin provided NaN values for more than 20 stations that might be a source of error in Table 3.6. In addition, the observations with ilogical precipitation (>100 [mm]) and wind speed (>30 [$^{m}/_{sec}$]) values are excluded. As a result, CRREL model can provide more accurate and reliable prediction. To develop the extreme freezing rain map, there is a need to perform advanced statistical analyses and estimate the maximum annual ice accretion with 50 years return period. As the climatological data is spatiotemporal, fitting marginal distribution function and estimation of its corresponding parameters must be done independently for each station. In other words, it is assumed that the freezing rain in each station is independent from its neighbour stations. However, this assumption might reduce robustness of the results, it decreases the complexity of the process. To develop extreme freezing rain events, a novel approach is developed. The involved steps are: (1) estimation of maximum accumulated ice accretion based on the site-specific historical icing data, (2) perform special interpolation, (3) compute the residuals, (4) conduct sensitivity analysis to

identify the effect geographical parameters on residuals, (5) fit a metaheuristic-based feedforward neural network to residuals and estimate residuals across the domain, (6) adding residuals to maximum ice values estimations, and (7) compute the concurrent wind speed.

- Estimation of maximum annual accumulated ice accretion based on the site-specific historical icing data: there are several studiues in the literature (e.g., (Jones et al., n.d.)) which employed Peak-Over-Threshold and Gumbel distribution to estimate the maximum annual ice accretion with 50years return period. Sheng et. al(Sheng et al., 2023) revealed that Gumebl distribution and Log-normal distribution are preferred for regions with high and moderate or low ice accretion, respectively. Herein, three distributions, namely Log-normal distribution, Gumbel distribution, and Generalized extreme distribution, are employed for fitting. The selection mechanism is designed and implemented based maximum likelihood approach. Figure 3.12 depicts the frequency of fitted distribution for maximum annual for different employed ice prediction model.

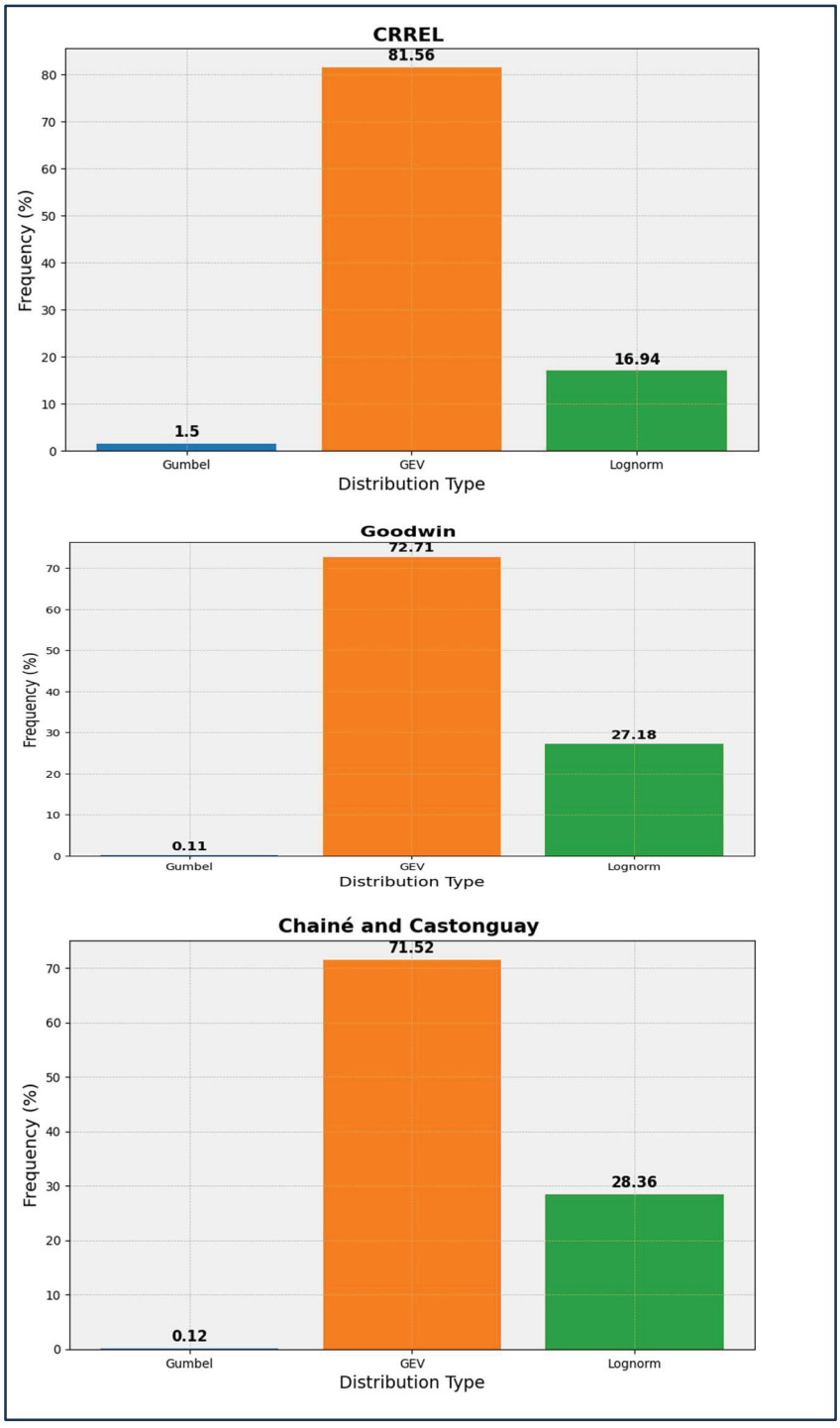

Figure 3.12 Frequency of fitted distributions for different ice prediction models

As Figure 3.12 Gumbel distribution is selected for few stations whereas GEV and Log-normal distributions are chosen the more.

- Perform special interpolation: to do spatial interpolation, Kriging spatial interpolation approach with nugget non-zero is utilized(Johnston et al., 2003). Kriging is a geostatistical interpolation technique that estimates unknown values by modelling the spatial correlation structure of the data through a variogram, which describes how sample values relate over distance. Kriging provides best linear unbiased predictions (BLUP) by weighting nearby observations, ensuring minimal prediction error variance. A nonzero nugget effect in a variogram model accounts for the small-scale variability or measurement error that cannot be captured at the sampling scale. By evaluating the estimations distributions and uncertainty of each model (i.e., standard deviation), spherical variogram (see Eq. (3.34)) was selected.

$$\gamma(h) = \begin{cases} 0 & h = 0 \\ C_0 + C\left(\frac{3}{2}\frac{h}{a} - \frac{1}{2}\frac{h^3}{a^3}\right) & 0 \le h \le a \\ C_0 + C & h > a \end{cases} \tag{3.34}$$

Where, C_0 = nugget constant, a = effective range, and C= the structure variance.

- Compute the residuals: The difference between the target values and estimations in stations are used as output for training the feedforward neural network.

- Conduct sensitivity analysis to identify the effect geographical parameters: In order to acquire a robust and reliable predictive model, it is crucial to do parameter selection. Threre are several approaches avaliable in the literature, such as backward elimination. The methodology utilized in this study revolves around the total Sobol indices, which are critical in sensitivity analysis for determining each input variables' contribution to an output variable's variance within a mathematical model. Sobol indices decompose

variance to illustrate how individual inputs and their interactions influence the model's output, thereby highlighting the importance of each factor. The first-order Sobol index measures the direct effect of a single input variable on the output variance, reflecting its primary influence. Conversely, the total Sobol index encompasses both the individual and interactive effects of an input variable on the output variance. This study employed a technique based on polynomial chaos expansion(Crestaux et al., 2009; Xiu & Karniadakis, 2003) to estimate the total Sobol indices. Polynomial chaos (PC) is an approach used in uncertainty quantification, representing random variables and their effects on system outputs through a series of orthogonal polynomials. These polynomials, tailored to the probability distribution of input uncertainties, form a basis that enables the expansion of outputs as sums of polynomial terms. Consequently, PC offers a structured method to approximate the influence of input uncertainties on model outputs, facilitating efficient computation of statistical moments and sensitivity indices. The following table lists the total sobol indicies obtained from PC expansion. A threshold of five percent was set for selection of effective parameters.

Table 3.7 Calculated Sobol indices obtained from PC expansion

Parameter	CRREL	Goodwin	Chainé and Castonguay
Longitude	29.45%	35.05%	3.23%
Latitude	21.81%	39.07%	70.21%
Elevation	48.74%	25.88%	26.56%

As Table 3.7 implies, easting is not important for Chainé and Castonguay model, however all parameters are important for CRREL and Goodwin.

- Fit a feedforward neural network to residuals and estimate residuals across the domain: To make predictions more accurate, a neural network model is fitted to the residuals and geological parameters to uncover the relationship between the residuals and

location of stations (e.g., northing and easting). The selected neural network model is a feedforward neural network. Feedforward neural networks (FNNs)(M. Shabani et al., 2022; Snaiki et al., 2024) consist of an input layer, one or more hidden layers, and an output layer, where each layer contains multiple neurons. The architecture is designed such that information flows in one direction—from the input nodes, through the hidden layers, and finally to the output nodes—without forming any cycles or loops. Despite their widespread application, FNNs trained with gradient-based optimizers, such as gradient descent, often encounter issues like local minima entrapment, vanishing gradients, and slow convergence. These limitations can hinder the network's performance and training efficiency. Metaheuristic optimizers, such as genetic algorithms or particle swarm optimization, offer a promising alternative by exploring the solution space more broadly and avoiding the pitfalls of gradient-based methods. Consequently, metaheuristic approaches can enhance the robustness and effectiveness of training feedforward neural networks. Grey wolf optimizer is selected for optimizing the FNNs because of its effectiveness and simplicity. The Grey Wolf Optimizer (GWO)(S. M. Mirjalili et al., 2014) is a nature-inspired optimization algorithm that mimics the social hierarchy and hunting behaviour of grey wolves. In GWO, a pack of wolves represents a population of candidate solutions. The wolves are categorized into four groups: alpha, beta, delta, and omega. The alpha wolves lead the pack in tasks such as hunting, feeding, and migration. Beta wolves act as subordinates, assisting the alpha in its duties. Delta and omega wolves are the lower ranks in the hierarchy, following orders and participating in the hunt. The hunting process, which inspires this optimization algorithm, includes three primary steps: 1. tracking and approaching the prey, 2. encircling and harassing the prey until it succumbs, and 3. attacking the prey.

- To train the metaheuristic-based FNN, a splitting ratio of 75%, 15% and 15% for training, testing and validation set is selected, respectively. The activation function is assumed to be ReLU, scaler = Minmax ($x_{scaled} = \frac{x - x_{min}}{x_{max} - x_{min}}$), batch size = 16, loss function = MSE, and epoch = 400. An early stopping mechanism (patience = 10 epochs

and minimum delta = 1e-4) is implemented to prevent overfitting of the network. Regarding the optimizer, this setup is selected: population = 50 agents and initialization range = [-100, 100]. The obtained MSE (R^2) values for training and testing sets are 2.28e-3 (88.79%) and 3.98e-3 (83.02%), respectively. The metrics indicate the model is trained properly and can be used for different applications.

- Adding residuals to maximum ice values estimations: Once the FNNs is trained properly, the residuals will be estimated across the domain and will be added to the fitted Kriging's prediction. It is of great importance to note that the resolution (i.e., mesh size) of the map must be determined before conducting the spatial interpolation. The developed map is depicted in following.

- Compute the concurrent wind speed: The most concerning part of developing extreme freezing rain map is to estimate the realistic value of concurent wind speed. Canadian Highway Bridge Design Code (CHBDC) recommends a scaling factor of 0.7 instead of performing statistical analysis. Jones et. al(Jones et al., n.d.) recommends that wind speed during an extreme freezing rain (V_{ext-}) event can be computed based on the T-year return period wind-induced load on an iced surface (e.g., transmission lines).

$$V_{ext-fr} = \sqrt{\frac{1}{\rho_{air} * C_{drag} d_{bare}} \frac{1}{\left(1+2*\frac{A_{ext,iced}}{d_{bare}}\right)}} \tag{3.35}$$

Where, ρ_{air} = density of air, C_{drag} = drag coefficient, $A_{ext,iced}$ = corss-sectional area of the iced surface, and $d_{cond,bare}$ = diameter of the surface without ice deposit. Therefore, it is employed for computing the concurrent wind speed during extreme freezing rain events.

3.7.1.4 Risk assessment

Similar to previous section (section 3.1.1.4), the trained neural network trained based on icing wind tunnel test results is utilized for prediction of drag coefficient. In addition, the obtained mathematical expression from SINDy is utilized for obtaining structural strain in lines. Moreover, importance sampling based on FOSM estimation is employed for solving Eq. (3.7). Angle of attack is assumed to be at its worst condition (i.e., 170°)(Rossi et al., 2020). Termination trigger mechanism is set activated once one of the following conditions is fulfilled:

- Reaching to the maximum number of sample (1,000,000 samples); or
- Coefficient of variation of obtained probabilities becomes less than a specified threshold.

The code was executed on an Intel Core i7-12700H processor and 16 GB of DDR5 RAM that took approximately more than 4,500 seconds.

As it was discussed before, one of the issues in integration of the PBFRE in design of extensive transmission system (i.e., at spatial scale) could be the extremely intensive computational cost required for solving the Eq. (3.7). For instance, let's assume that solving the Eq. (3.7) and achieving a reliable value takes about 10 seconds for a single point. Therefore, the total time for solving the equation for more than 900 stations will be 9,000 seconds. If the design process needs to be repeated 50 times for optimizing the desired parameters (e.g., shape) the runtime will jump to will be 4,500,000 seconds (i.e., 52 days). A metaheuristic-based ANN FNNs is designed for regenerating the maps and measure its performance in terms of different metrics, such as error, predictability and prediction time. The selected optimizer is whale optimizer which is a nature-inspired metaheuristic optimization algorithm that is based on bubble-net hunting mechanism of humpback whales(S. Mirjalili & Lewis, 2016). The Whale optimizer provides more advantages compared to its rivals, including fast convergence, fewer operators, better balance between exploration and exploitation phases and wider diversity due to spiral

updating mechanism. The updating procedure of the Whale optimizer is presented in following.

$$X^{j+1} = \begin{cases} \vec{X^j_{best}} - \vec{A}.\vec{D}, & if\ p < 0.5\ and\ |A| < 1 \\ D.exp(const * l).\cos(2\pi l) + \vec{X^j_{best}}, & if\ p \geq 0.5\ and\ |A| < 1 \\ \vec{X_{rand}} - \vec{A}.\vec{D}, & if\ |A| \geq 1 \end{cases} \quad (3.36)$$

where, X^j_{best}= the best position found so far, $p =$ random number, and $l =$ constant value. In Eq. (36), $|A| < 1$ implies the exploitation phases and $|A| \geq 1$ denotes the exploration phase. The network's architecture is listed in Table 3.8.

Table 3.8 Deep learning architecture for prediction of risk levels

Param	Value
Inputs size	2
Output size	3
Hidden layer	2
Number of neurons	64-36
Optimizer	Whale optimizer
Epoch	400
Populations	50 agents
Training split ratio	70%
Scaler	MinMax

To obtain the optimized weights and biases, the network is trained based on pseudo-values generated by solving the Eq. (3.7) using the importance sampling simulator. The inputs are assumed to be transparent, solid and dense ice accretion (i.e., glaze) thickness and 3-seconds gust wind speed. 20 ice samples and 20 3-seconds gust wind speed are mixed together to create

400 combinations. The obtained MSE and R^2 for training and testing are 3e-3, 91.38%, 2e-2 and 83.9%, respectively. The results imply that the mode is trained properly and can be applied for predicting of freezing rain-induced risk at spatial scale. As it was mentioned before, the angle of attack is assumed to be $170°$ that indicate the worst condition for onset and propagation of instabilities in conductors. To evaluate the proposed novel machine learning-based framework's performance, MSE and R^2 of generated maps are computed and reported in the following table.

Table 3.9 Computed metrics for testing the performance of the novel machine learning-based framework

Risk level	MSE	R^2
Slight	0.003	95.8%
Moderate	0.018	76.3%
Extensive	0.055	69.3%

The results in Table 3.9 indicate that the machine learning based framework is quite accurate and can be employed for prediction of the freezing rain-induced risk levels. In addition, the results demonstrate that although the importance sampling simulator based FOSM estimation needs at least 4,500 seconds to generate the risk maps while machine learning-based framework need almost less than one second (99.97% decrease in processing time). Consequently, different machine learning models can be readily integrated into the framework for prediction.

3.7.1.5 Accounting for variability in climatological patterns

Another concerning point in the framework is how to account for the change in climatological patterns (e.g., climate change effect). To address this issue, Internet of Things (IoT) principles can be used. In other words, real-time prediction of climatological patterns was impossible until the last decades that a dense network of sensors was installed to measure and record

weather parameters, such as precipitation rate, precipitation type, accreted ice, wind speed and gust wind speed. Therefore, it can be readily integrated into the PBFRE framework to overcome this limitation. To illustrate its application, the historical site specific from few stations, namely (DECORAH and Olympia) are collected from clean dataset, mentioned in section 1.1.9.1.1 & 1.1.9.1.2. It should be noted that the CRREL model is used for prediction of ice accretion. The extreme ice accretion is estimated using the approach in section 1.1.9.1.2 and then Naïve Bayes approach principle is used for prediction of freezing rain event with 50 years return period. The prior and posterior distributions are assumed to be same as the ones which are selected in the novel approach. The results are presented in the following table.

Table 3.10 Obtained maximum ice accretion with and without considering the change of climatological patterns

Station	**Ice max obtained by**	
	Novel approach (mm)	**Naïve Bayes method (mm)**
DECORAH	3.855	3.853
Olympia	3.905	4.017

As Table 3.10 indicate, the change in prediction of extreme ice accretion for the first station might be significant; however, in the second the change is about 2.861%. This change may be so small, even though it could be extremely important when it comes to calculating the ice accretion-induced loads. The estimated ice weight in the second station is 3.26% higher than the first approach for same wind speed and drag coefficient, whereas this change is 0.03% less for the first stations. As a result, it can be clearly seen that considering these changes is crucial at early design steps and PBFRE framework has the potential to account for that. Moreover, other advanced numerical methodologies can be readily integrated into the framework for capturing these variations more accurately to optimize the design. Under extreme conditions such as power outages or hardware failures during freezing rain events, IoT sensors and ML

models can maintain performance through several resilience-enhancing strategies. IoT systems can incorporate redundancy by deploying multiple sensors to ensure data collection continuity if some devices fail. They can also utilize energy-efficient designs, such as low-power modes and backup batteries, to function during power disruptions. Edge computing allows localized data processing to reduce reliance on central servers, mitigating the impact of connectivity issues. For ML models, adaptive algorithms can handle missing or partial data by imputing values based on historical trends or real-time patterns. Combining these strategies with fault-tolerant communication protocols and cloud-based backups ensures robust data collection, processing, and analysis even under adverse conditions.

3.8 Conclusion

In this study, an innovative Performance-Based Freezing Rain Engineering (PBFRE) framework was introduced. The PBFRE can be readily integrated into design schemes or devising maintenance plans of structural systems in cold regions. The framework is designed to be employed at different scales, namely structural and spatial. As a result, it has the potential to facilitate development of an early warning system to minimize freezing rain-induced risk. At structural scale, it is disaggregated into different small tasks, namely hazard analysis, structural characterizations, interaction analysis, structural analysis, damage analysis, loss analysis, and decision making. Despite previously developed frameworks, the PBFRE framework leverages the principles of Internet of Things and Machine learning to address challenges of freezing rain-induced risk forecasting, especially time varying climatological patterns, extensive computational cost, complexity and interaction between several hazards. The PBFRE framework was illustrated through a case study application for prediction of freezing rain-induced risk to a tower-line transmission system in the USA. The application of the framework for both design and maintenance was illustrated. At structural scale, Eq. (3.7) was solved based on a deviation of Monte Carlo Sampling for a FE model subjected to glaze ice and wind actions. In addition, an advanced surrogate model based on sparsity was integrated to showcase the flexibility of the framework. In the spatial scale, a comprehensive

investigation was carried out to highlight the effect of using different ice prediction models and a novel approach for development of extreme freezing rain event was developed. Moreover, the importance of utilizing Internet of Things for developing real-time prediction was explained. The results indicated the effectiveness and accuracy of the PBFRE framework for prediction of freezing rain risk to infrastructures.

CONCLUSION

In this study, a thorough review of the existing literature was conducted to identify gaps in the field of freezing rain impact assessment. This review informed the development of the PBE framework and contributed to the broader academic discourse by highlighting areas where further research is necessary.

Various ice prediction models were evaluated and compared to determine their effectiveness in predicting glaze ice formation. The study identified the Cold Regions Research and Engineering Laboratory (CRREL) model as the most accurate, providing a critical benchmark for future research and practical applications.

This research introduced a specialized Performance-Based Engineering framework for assessing the risks faced by electrical grids subjected to glaze ice. The framework specifically addressed the phenomenon of galloping in power lines, thereby enhancing the grid's resilience and reliability under extreme weather conditions.

The study conducted a detailed risk assessment across two scales—spatial and structural—at two critical time steps in the structural lifecycle: the early design phase and the maintenance phase. This dual-scale, time-dependent analysis provided deeper insights into the impacts of freezing rain on the grid throughout its lifecycle, informing both design and maintenance strategies.

The thesis developed two limit state functions specifically designed to address the problem of galloping in electrical grids. These functions are essential components of the risk assessment framework, allowing for precise evaluation of the conditions under which galloping may occur and its potential consequences.

The study conducted a detailed risk assessment across two scales—spatial and structural—at two critical time steps in the structural lifecycle: the early design phase and the maintenance phase. This dual-scale, time-dependent analysis provided deeper insights into the impacts of freezing rain on the grid throughout its lifecycle, informing both design and maintenance strategies.

The thesis developed a specialized Performance-Based Engineering framework focused on addressing the challenges posed by freezing rain events, particularly galloping in structural systems. By integrating Internet of Things technology, the framework enabled real-time monitoring and more accurate predictions, enhancing its effectiveness in mitigating risks. Additionally, machine learning algorithms were employed to optimize computational processes, allowing for faster and more efficient predictions. This interdisciplinary approach significantly advanced the design and management of resilient infrastructure in cold climates, contributing to the broader field of structural resilience.

RECOMMENDATIONS

As we transition from the theoretical findings and in-depth analysis of this study to practical applications, it's essential to outline a roadmap for the future development of a Performance-Based Engineering framework tailored to freezing rain events. Based on our research outcomes, we propose the following strategies to enhance the implementation of PBE in addressing freezing rain impacts on structural systems. These recommendations are designed to fill the identified gaps, tackle existing challenges, and fully harness the potential of PBE in both design and maintenance phases.

The goal is to equip engineers, researchers, and policymakers with actionable insights that promote innovation, encourage interdisciplinary collaboration, and drive progress in resilience-based design. By adopting these strategies, the benefits of a PBE approach can be scaled effectively, contributing significantly to the advancement of engineering practices under extreme weather conditions. The following recommendations are crafted to turn the theoretical insights of this study into practical, impactful measures for improving structural resilience to freezing rain events.

1) **Utilizing Diverse Data Sources**: In addition to ASOS data, incorporating data from other weather stations or sources could improve the robustness of the predictions. This would allow for a more comprehensive evaluation of the framework's effectiveness across different conditions and regions.

2) **Applying Accurate Prediction Models**: Employing more precise models, such as the ISO 12494 standard, which is specifically designed for atmospheric icing, could lead to better accuracy in predicting glaze ice characteristics. This model considers various factors influencing ice accretion, providing a more reliable prediction.

3) **Conducting Icing Wind Tunnel Tests**: Performing wind tunnel experiments that simulate icing conditions can yield detailed insights into the shape of ice formations and the relationship between wind speed, direction, and ice accretion. This empirical data could be used to validate and refine the predictive models.

4) **Exploring Different Angles of Attack**: Investigating how varying angles of attack influence ice accretion could reveal critical insights, especially for structures like power lines and wind turbines. Understanding these effects can help in developing more effective mitigation strategies.

5) **Incorporating Advanced Climate Change Scenarios**: Testing the framework under advanced climate change scenarios would provide valuable information on its applicability and reliability in future conditions. This approach would also help in understanding the potential impacts of climate change on glaze ice formation and accumulation.

Implementing these recommendations could lead to more accurate and reliable predictions, ultimately improving the effectiveness of the framework in real-world applications.

LIST OF BIBLIOGRAPHICAL REFERENCES

Arriaga, D. D. (2020). *Joint Wind and Ice Effects on Transmission Lines in Mountainous Joint Wind and Ice Effects on Transmission Lines in Mountainous Terrain Terrain*. University of Western Ontario.

Attary, N., Van De Lindt, J. W., Barbosa, A. R., Cox, D. T., & Unnikrishnan, V. U. (2021). Performance-Based Tsunami Engineering for Risk Assessment of Structures Subjected to Multi-Hazards: Tsunami following Earthquake. *Journal of Earthquake Engineering*, *25*(10), 2065–2084. https://doi.org/10.1080/13632469.2019.1616335

Augusti, G., & Ciampoli, M. (2008). Performance-Based Design in risk assessment and reduction. *Probabilistic Engineering Mechanics*, *23*(4), 496–508. https://doi.org/10.1016/j.probengmech.2008.01.007

Augusti, G., Paulotto, C., & Ciampoli, M. (n.d.). Some proposals for a first step towards a Performance Based Wind Engineering. *International Journal Canada s Journal of Global Policy Analysis*. https://www.researchgate.net/publication/228826913

Barbato, M., Petrini, F., Unnikrishnan, V. U., & Ciampoli, M. (2013). Performance-Based Hurricane Engineering (PBHE) framework. *Structural Safety*, *45*, 24–35. https://doi.org/10.1016/j.strusafe.2013.07.002

Behrens, J., Løvholt, F., Jalayer, F., Lorito, S., Salgado-Gálvez, M. A., Sørensen, M., Abadie, S., Aguirre-Ayerbe, I., Aniel-Quiroga, I., Babeyko, A., Baiguera, M., Basili, R., Belliazzi, S., Grezio, A., Johnson, K., Murphy, S., Paris, R., Rafliana, I., De Risi, R., … Vyhmeister, E. (2021). Probabilistic Tsunami Hazard and Risk Analysis: A Review of Research Gaps. *Frontiers in Earth Science*, *9*. https://doi.org/10.3389/feart.2021.628772

Best, A. C. (1950). The size distribution of raindrops. *Quarterly Journal of the Royal Meteorological Society*, *76*(327), 16–36. https://doi.org/10.1002/qj.49707632704

Borna, A. (2014). *Prediction of Galloping of Transmission Line Conductors by a Computational Aeroelastic Approach*. McGill University.

Brown, C. M., Kunz, R. F., Kinzel, M. P., Lindau, J., Palacios, J., & Brentner, K. S. (2014, June 16). Large Eddy Simulation of Airfoil Ice Accretion Aerodynamics. *6th AIAA*

Atmospheric and Space Environments Conference. https://doi.org/10.2514/6.2014-2203

Brunton, S. L., Noack, B. R., & Koumoutsakos, P. (2020). Machine Learning for Fluid Mechanics. *Annual Review of Fluid Mechanics*, *52*(1), 477–508. https://doi.org/10.1146/annurev-fluid-010719-060214

Brunton, S. L., Proctor, J. L., & Kutz, J. N. (2016). Discovering governing equations from data by sparse identification of nonlinear dynamical systems. *Proceedings of the National Academy of Sciences*, *113*(15), 3932–3937. https://doi.org/10.1073/pnas.1517384113

Buchanan, A. H. (1994). Fire engineering for a performance based code. *Fire Safety Journal*, *23*(1), 1–16. https://doi.org/10.1016/0379-7112(94)90058-2

Chainé, P. M., & Castonguay, G. (1974). New approach to radial ice thickness concept applied to bundle-like conductors. *Industrial Meteorology-Study IV, Environment Canada, Toronto*.

Chaîné, P. M., & Castonguay, G. (1974). New approach to radial ice thickness concept applied to bundle-like conductors. *Environment Canada, Atmospheric Environment*, *4*.

Chandler, A. M., & Lam, N. T. K. (2001). Performance-based design in earthquake engineering: a multi-disciplinary review. *Engineering Structures*, *23*(12), 1525–1543. https://doi.org/10.1016/S0141-0296(01)00070-0

Chang, S., Leng, M., Wu, H., & Thompson, J. (2016). Aircraft ice accretion prediction using neural network and wavelet packet transform. *Aircraft Engineering and Aerospace Technology*, *88*(1), 128–136. https://doi.org/10.1108/AEAT-05-2014-0057

Ciampoli, M., & Petrini, F. (2012). Performance-based Aeolian risk assessment and reduction for tall buildings. *Probabilistic Engineering Mechanics*, *28*, 75–84. https://doi.org/10.1016/j.probengmech.2011.08.013

Ciampoli, M., Petrini, F., & Augusti, G. (2011). Performance-Based Wind Engineering: Towards a general procedure. *Structural Safety*, *33*(6), 367–378. https://doi.org/10.1016/j.strusafe.2011.07.001

Cigré. (2006). *291 Guidelines for Meteorological Icing Models, Statistical Methods and Topographical Effects*. https://e-cigre.org/publication/291-guidelines-for-meteorological-icing-models-statistical-methods-and-topographical-effects

Crestaux, T., Le Maıˆtre, O., & Martinez, J.-M. (2009). Polynomial chaos expansion for sensitivity analysis. *Reliability Engineering & System Safety*, *94*(7), 1161–1172. https://doi.org/10.1016/j.ress.2008.10.008

CSA Group. (2020). *CSA C22.3 NO. 1:20 Overhead systems*.

Cui, W., & Caracoglia, L. (2018). A unified framework for performance-based wind engineering of tall buildings in hurricane-prone regions based on lifetime intervention-cost estimation. *Structural Safety*, *73*, 75–86. https://doi.org/10.1016/j.strusafe.2018.02.003

Davalos, D., Chowdhury, J., & Hangan, H. (2023). Joint wind and ice hazard for transmission lines in mountainous terrain. *Journal of Wind Engineering and Industrial Aerodynamics*, *232*, 105276. https://doi.org/10.1016/j.jweia.2022.105276

Deak, G., Curran, K., Condell, J., Asimakopoulou, E., & Bessis, N. (2013). IoTs (Internet of Things) and DfPL (Device-free Passive Localisation) in a disaster management scenario. *Simulation Modelling Practice and Theory*, *35*, 86–96. https://doi.org/10.1016/j.simpat.2013.03.005

Der Kiureghian, A. (2022). *Structural and System Reliability*. Cambridge University Press. https://doi.org/10.1017/9781108991889

Diem, M. (1956). Ice loads on high voltage lines in the mountains. *Arch. Mat. Geoph. Biokl. Ser. B*, *7*, 84–85.

Dorri, F., Hooman Ghasemi, S., & Jalilkhani, M. (2023). Performance-based system reliability analysis for steel moment frames. *Structures*, *51*, 472–483. https://doi.org/10.1016/j.istruc.2023.03.047

Druez, J., Louchez, S., & McComber, P. (1995). Ice shedding from cables. *Cold Regions Science and Technology*, *23*(4), 377–388. https://doi.org/10.1016/0165-232X(94)00024-R

Dwaipayan Sharma, Ahmed Abdelaal, & Douglas Nims. (2022, May 19). *A CFD Analysis of the Effect of Ice and Snow Accretion on the Aerodynamic Behavior of Bridge Cables*.

Esmaeili, M., & Barbato, M. (2022). Performance-Based Hurricane Engineering under Changing Climate Conditions: General Framework and Performance of Single-Family

Houses in the US. *Journal of Structural Engineering*, *148*(10). https://doi.org/10.1061/(ASCE)ST.1943-541X.0003447

FEMA Hazus-MH MR4. Multi-hazard loss estimation methodology: earthquake model, HAZUS-MH MR4: Technical manual. Washington DC: Federal Emergency Management Agency. (2003).

Fikke, S. M., Kristjánsson, J. E., & Kringlebotn Nygaard, B. E. (2008). Modern Meteorology and Atmospheric Icing. In M. Farzaneh (Ed.), *Atmospheric Icing of Power Networks* (pp. 1–29). Springer Netherlands. https://doi.org/10.1007/978-1-4020-8531-4_1

Finstad, K. J., Skjetne, R., & Mikkelsen, O. (2003). A simple model for ice accretion. *Proc. Tenth International Workshop on Atmospheric Icing of Structures*.

Fu, P., Farzaneh, M., & Bouchard, G. (2006). Two-dimensional modelling of the ice accretion process on transmission line wires and conductors. *Cold Regions Science and Technology*, *46*(2), 132–146. https://doi.org/10.1016/j.coldregions.2006.06.004

Fu, X., Li, H.-N., Li, G., & Dong, Z.-Q. (2020). Fragility analysis of a transmission tower under combined wind and rain loads. *Journal of Wind Engineering and Industrial Aerodynamics*, *199*, 104098. https://doi.org/10.1016/j.jweia.2020.104098

Goel, A. (n.d.). Design of Transmission Lines for Atmospheric Icing. In *Atmospheric Icing of Power Networks* (pp. 327–371). Springer Netherlands. https://doi.org/10.1007/978-1-4020-8531-4_8

Goodwin, E. J., Mozer, J. D., Jr, A. M. D. G., & Power, .B.A. (1983). Predicting ice and snow loads for transmission lines. *In Proceedings of the First International Workshop on Atmospheric Icing of Structures*, 267–273.

Gou, Y., Li, Q., Yao, R., Chen, J., Zhao, H., & Zhang, Z. (2023). Ice accretion existence and three-dimensional shape identification based on infrared thermography detection. *Infrared Physics & Technology*, *135*, 104972. https://doi.org/10.1016/j.infrared.2023.104972

Guerard, S., Godard, B., & Lilien, J.-L. (2011). Aeolian Vibrations on Power-Line Conductors, Evaluation of Actual Self Damping. *IEEE Transactions on Power Delivery*, *26*(4), 2118–2122. https://doi.org/10.1109/TPWRD.2011.2151211

H. M. Irvine, & T. K. Caughey. (1974). The linear theory of free vibrations of a suspended cable. *Proceedings of the Royal Society of London. A. Mathematical and Physical Sciences*, *341*(1626), 299–315. https://doi.org/10.1098/rspa.1974.0189

Hartog, J. P. Den. (1932). Transmission Line Vibration Due to Sleet. *Transactions of the American Institute of Electrical Engineers*, *51*(4), 1074–1076. https://doi.org/10.1109/T-AIEE.1932.5056223

Herbin, A. H., & Barbato, M. (2012). Fragility curves for building envelope components subject to windborne debris impact. *Journal of Wind Engineering and Industrial Aerodynamics*, *107–108*, 285–298. https://doi.org/10.1016/j.jweia.2012.05.005

Heresi, P., & Miranda, E. (2023). RPBEE: Performance-based earthquake engineering on a regional scale. *Earthquake Spectra*, *39*(3), 1328–1351. https://doi.org/10.1177/87552930231179491

Huang, Z., Rosowsky, D. ., & Sparks, P. . (2001). Hurricane simulation techniques for the evaluation of wind-speeds and expected insurance losses. *Journal of Wind Engineering and Industrial Aerodynamics*, *89*(7–8), 605–617. https://doi.org/10.1016/S0167-6105(01)00061-7

Jalayer, F., & Cornell, C. A. (2004). *A technical framework for probability-based demand and capacity factor design (DCFD) seismic formats*.

Jasinski, W. J., Noe, S. C., Selig, M. S., & Bragg, M. B. (1998). Wind Turbine Performance Under Icing Conditions. *Journal of Solar Energy Engineering*, *120*(1), 60–65. https://doi.org/10.1115/1.2888048

Jianwei Wang, & Lilien, J.-L. (1998). Overhead electrical transmission line galloping. A full multi-span 3-DOF model, some applications and design recommendations. *IEEE Transactions on Power Delivery*, *13*(3), 909–916. https://doi.org/10.1109/61.686992

Johnston, K., Hoef, J. M. Ver, Konstantin, K., & Lucas, N. (2003). *Using ArcGI S Geostatistical Analyst*. academia.edu.

Jones, K. F. (1996a). A simple model for freezing rain ice loads. *Proc. Seventh International Workshop on Atmospheric Icing of Structures*, 412–416.

Jones, K. F. (1996b). *Ice accretion in freezing rain* (Issues 96–2).

Jones, K. F. (1998). A simple model for freezing rain ice loads. *Atmospheric Research*, *46*(1–2), 87–97. https://doi.org/10.1016/S0169-8095(97)00053-7

Jones, K. F. (2023). An analysis of the basis of the Chaîné model for ice accretion in freezing rain. *Cold Regions Science and Technology*, *209*, 103820. https://doi.org/10.1016/j.coldregions.2023.103820

Jones, K. F., Ramsay, A. C., & Lott, J. N. (2004). Icing Severity in the December 2002 Freezing-Rain Storm from ASOS Data*. *Monthly Weather Review*, *132*(7), 1630–1644. https://doi.org/10.1175/1520-0493(2004)132<1630:ISITDF>2.0.CO;2

Jones, K. F., Thorkildson, R., & Lott, J. N. (n.d.). *The development of the map of extreme ice loads for ASCE Manual 74*. www.americanlifelinesalliance.org

K.F. Jones. (1996). *Ice Accretion in Freezing Rain*.

Kämäräinen, M., Hyvärinen, O., Vajda, A., Nikulin, G., Meijgaard, E. van, Teichmann, C., Jacob, D., Gregow, H., & Jylhä, K. (2018). Estimates of Present-Day and Future Climatologies of Freezing Rain in Europe Based on CORDEX Regional Climate Models. *Journal of Geophysical Research: Atmospheres*, *123*(23). https://doi.org/10.1029/2018JD029131

Koh, C. G., & See, L. M. (1994). Identification and Uncertainty Estimation of Structural Parameters. *Journal of Engineering Mechanics*, *120*(6), 1219–1236. https://doi.org/10.1061/(ASCE)0733-9399(1994)120:6(1219)

Kong, S., Cui, H., Tian, Y., & Ji, S. (2020). Identification of ice loads on shell structure of ice-going vessel with Green kernel and regularization method. *Marine Structures*, *74*, 102820. https://doi.org/10.1016/j.marstruc.2020.102820

Kyburz, M. L., Sovilla, B., Gaume, J., & Ancey, C. (2022). Physics-based estimates of drag coefficients for the impact pressure calculation of dense snow avalanches. *Engineering Structures*, *254*, 113478. https://doi.org/10.1016/j.engstruct.2021.113478

Lecomte, E. L., Pang, A. W., & Russell, J. W. (1998). Ice Storm "98." *Institute for Catastrophic Loss Reduction, Ottawa, ON, Canada and Institute for Business and Home Safety, Boston, MA, USA*, *1*, 47.

Li, P., Li, N., Li, Q., CAO, M., & CHEN, H. (2010). Prediction Model for Power Transmission

Line Icing Load Based on Data-Driven. *Advanced Materials Research*, *143–144*, 1295–1299. https://doi.org/10.4028/www.scientific.net/AMR.143-144.1295

Li, Y., & Ellingwood, B. R. (2006). Hurricane damage to residential construction in the US: Importance of uncertainty modeling in risk assessment. *Engineering Structures*, *28*(7), 1009–1018. https://doi.org/10.1016/j.engstruct.2005.11.005

Liel, A., Jackson, K., & Geis, J. (2011). A framework for performance-based design and assessment of buildings subjected to extreme snow loads. In *Applications of Statistics and Probability in Civil Engineering* (pp. 924–931). CRC Press. https://doi.org/10.1201/b11332-139

Lilien, J.-L., Van Dyke, P., Asselin, J.-M., Farzaneh, M., Halsan, K., Havard, D., Hearnshaw, D., Laneville, A., Mito, M., Rawlins, C. B., St-Louis, M., Sunkle, D., & Vinogradov, A. (2005). *State of the art of conductor galloping. Task Force B2.11.06*.

Liu, X., Chen, L., Ye, Z., Zhang, B., & Tao, Y. (2023). Data-driven sparse identification of galloping model of iced quad bundle conductors. *Measurement*, *207*, 112356. https://doi.org/10.1016/j.measurement.2022.112356

Lu, J., Wang, Q., Wang, L., Mei, H., Yang, L., Xu, X., & Li, L. (2019). Study on wind tunnel test and galloping of iced quad bundle conductor. *Cold Regions Science and Technology*, *160*, 273–287. https://doi.org/10.1016/j.coldregions.2018.12.009

Mackie, K. R., Wong, J.-M., & Stojadinovic, B. (2009). Seismic Risk Evaluation for the Baseline PEER Bridge Testbed. *TCLEE 2009*, 1–12. https://doi.org/10.1061/41050(357)58

Macklin, W. C. (1962). The density and structure of ice formed by accretion. *Quarterly Journal of the Royal Meteorological Society*, *88*(375), 30–50. https://doi.org/10.1002/qj.49708837504

Makkonen, L. (1984). Modeling of Ice Accretion on Wires. *Journal of Climate and Applied Meteorology*, *23*(6), 929–939. https://doi.org/10.1175/1520-0450(1984)023<0929:MOIAOW>2.0.CO;2

Makkonen, L. (1998). Modelling power line icing in freezing precipitation. *Atmospheric Research*, *46*, 131–142.

Makkonen, L. (2000). Models for the growth of rime, glaze, icicles and wet snow on structures. *Philosophical Transactions of the Royal Society of London. Series A: Mathematical, Physical and Engineering Sciences*, *358*(1776), 2913–2939. https://doi.org/10.1098/rsta.2000.0690

Makkonen, L., & Stallabrass, J. R. (1984). *Ice accretion on cylinders and wires* (Issue TR-LT-005).

Marshall, J. S., & Palmer, W. M. K. (1948). The distribution of raindrops with size. *Journal of Atmospheric Sciences*, *5*(4), 165–166.

McClure, G., Johns, K., Knoll, F., & Pichette, G. (2002). Lessons from the ice storm of 1998: Improving the structural features of Hydro-Quebec's power grid. *10th International Workshop on Atmospheric Icing*.

McComber, P. (1984). Numerical simulation of cable twisting due to icing. *Cold Regions Sci. Technol.*, *8*, 253–259.

McComber, P., & Paradis, A. (1998). A cable galloping model for thin ice accretions. *Atmospheric Research*, *46*(1–2), 13–25. https://doi.org/10.1016/S0169-8095(97)00047-1

Meng, X., Tian, L., Li, C., & Liu, J. (2024). Copula-based wind-induced failure prediction of overhead transmission line considering multiple temperature factors. *Reliability Engineering & System Safety*, *247*, 110138. https://doi.org/10.1016/j.ress.2024.110138

Mirjalili, S., & Lewis, A. (2016). The Whale Optimization Algorithm. *Advances in Engineering Software*, *95*, 51–67. https://doi.org/10.1016/j.advengsoft.2016.01.008

Mirjalili, S. M., Mirjalili, S. M., & Lewis, A. (2014). Grey Wolf Optimizer. *Advances in Engineering Software*, *69*, 46–61. https://doi.org/10.1016/j.advengsoft.2013.12.007

Nussen, R. P. L., & Van Delft, D. R. V. (2003). *Alternative Fatigue Formulations for Variable Amplitude Loading of Fibre Composites for Wind Turbine Rotor Blades* (pp. 563–574). https://doi.org/10.1016/S1566-1369(03)80125-5

Nygaard, B. E. K., Seierstad, I. A., & Veal, A. T. (2014). A new snow and ice load map for mechanical design of power lines in Great Britain. *Cold Regions Science and Technology*, *108*, 28–35. https://doi.org/10.1016/j.coldregions.2014.09.001

Ogretim, E., Huebsch, W., & Shinn, A. (2006). Aircraft Ice Accretion Prediction Based on

Neural Networks. *Journal of Aircraft*, *43*(1), 233–240. https://doi.org/10.2514/1.16241

Ouyang, Z., & Spence, S. M. J. (2021). A Performance-Based Wind Engineering Framework for Engineered Building Systems Subject to Hurricanes. *Frontiers in Built Environment*, *7*. https://doi.org/10.3389/fbuil.2021.720764

Pohlman, J., & Landers, P. (1982). Present State-of-the-Art of Transmission Line Icing. *IEEE Transactions on Power Apparatus and Systems*, *PAS-101*(8), 2443–2450. https://doi.org/10.1109/TPAS.1982.317605

Poots, G., & Skelton, P. L. I. (1994). Simple models for wet-snow accretion on transmission lines: snow load and liquid water content. *International Journal of Heat and Fluid Flow*, *15*(5), 411–417. https://doi.org/10.1016/0142-727X(94)90055-8

Poots, G., & Skelton, P. L. I. (1995). Simulation of wet-snow accretion by axial growth on a transmission line conductor. *Applied Mathematical Modelling*, *19*(9), 514–518. https://doi.org/10.1016/0307-904X(95)00012-9

Porter, K. A. (2003). An overview of PEER's performance-based earthquake engineering methodology. *Proceedings of Ninth International Conference on Applications of Statistics and Probability in Civil Engineering*, 1–8.

Porter, K. A., Kiremidjian, A. S., & LeGrue, J. S. (2001). Assembly-Based Vulnerability of Buildings and Its Use in Performance Evaluation. *Earthquake Spectra*, *17*(2), 291–312. https://doi.org/10.1193/1.1586176

Rini, D., & Lamont, S. (2008). Performance Based Structural Fire Engineering for Modern Building Design. *Structures Congress 2008*, 1–12. https://doi.org/10.1061/41016(314)248

Rojas, R. (1996). The Backpropagation Algorithm. In *Neural Networks* (pp. 149–182). Springer Berlin Heidelberg. https://doi.org/10.1007/978-3-642-61068-4_7

Rossi, A., Jubayer, C., Koss, H., Arriaga, D., & Hangan, H. (2020). Combined effects of wind and atmospheric icing on overhead transmission lines. *Journal of Wind Engineering and Industrial Aerodynamics*, *204*, 104271. https://doi.org/10.1016/j.jweia.2020.104271

Rudzinski, W. J., Farzaneh, M., & Lozowski, E. P. (2005). Full-scale 3D numerical and laboratory simulations of glaze ice accretion on a non-energized station post insulator.

Proc. Eleventh International Workshop on Atmospheric Icing of Structures.

SCRUTON, C., & FLINT, A. R. (1964). WIND-EXCITED OSCILLATIONS OF STRUCTURES. *Proceedings of the Institution of Civil Engineers*, *27*(4), 673–702. https://doi.org/10.1680/iicep.1964.10179

Scuro, C., Sciammarella, P. F., Lamonaca, F., Olivito, R. S., & Carni, D. L. (2018). IoT for structural health monitoring. *IEEE Instrumentation & Measurement Magazine*, *21*(6), 4–14. https://doi.org/10.1109/MIM.2018.8573586

Seyedeh Nasim Rezaei. (2016). *FRAGILITY ASSESSMENT AND RELIABILITY ANALYSIS OF TRANSMISSION LINES SUBJECTED TO CLIMATIC HAZARDS*. University of McGill.

Shabani, M., Jamali;, A., Snaiki, R., & Rahem, A. (2022, May). Prediction of Ice Accretion on Transmission Lines using Hybrid Particle Swarm Optimization-based Artificial Neural Networks. *Int. Workshop on Atmospheric Icing of Structures (IWAIS2022)*.

Shabani, M. M., Taheri, A., & Daghigh, M. (2017). Reliability assessment of free spanning subsea pipeline. *Thin-Walled Structures*, *120*, 116–123. https://doi.org/10.1016/j.tws.2017.08.026

Sheng, C., Tang, Q., & Hong, H. P. (2023). Estimating and Mapping Extreme Ice Accretion Hazard and Load Due to Freezing Rain at Canadian Sites. *International Journal of Disaster Risk Science*, *14*(1), 127–142. https://doi.org/10.1007/s13753-023-00466-1

Snaiki, R. (2024). Performance-based ice engineering framework: A data-driven multi-scale approach. *Cold Regions Science and Technology*, *224*, 104247. https://doi.org/10.1016/j.coldregions.2024.104247

Snaiki, R., Jamali, A., Rahem, A., Shabani, M., & Barjenbruch, B. L. (2024). A metaheuristic-optimization-based neural network for icing prediction on transmission lines. *Cold Regions Science and Technology*, *224*, 104249. https://doi.org/10.1016/j.coldregions.2024.104249

Snaiki, R., & Shabani, M. (2023). Performance-Based Ice Engineering: A Novel Multi-Scale Approach. *Canadian Society of Civil Engineering (CSCE) 2023*.

Snaiki, R., & Shabani, M. (2024). *Performance-Based Ice Engineering: A Novel Multi-Scale*

Approach. https://doi.org/10.48550/arXiv.2401.13860

Solangi, A. R. (2018). *Icing Effects on Power Lines and Anti-icing and De-icing Methods*. *June*, 1–99. https://ninum.uit.no/handle/10037/14198

Stallabrass, J. R., Hearty, P. F., & of Canada. Division of Mechanical Engineering, N. R. C. (1967). *The Icing of Cylinders in Conditions of Simulated Freezing Sea Spray*. National Research Council of Canada. https://books.google.ca/books?id=jjYlLTsRPrEC

Su, L., Wu, X., Zhang, X., & Huang, X. (2021). Smart performance-based design for building fire safety: Prediction of smoke motion via AI. *Journal of Building Engineering*, *43*, 102529. https://doi.org/10.1016/j.jobe.2021.102529

Thai, H.-T. (2022). Machine learning for structural engineering: A state-of-the-art review. *Structures*, *38*, 448–491. https://doi.org/10.1016/j.istruc.2022.02.003

Unnikrishnan, V. U., & Barbato, M. (2017). Multihazard Interaction Effects on the Performance of Low-Rise Wood-Frame Housing in Hurricane-Prone Regions. *Journal of Structural Engineering*, *143*(8). https://doi.org/10.1061/(ASCE)ST.1943-541X.0001797

Van Dyke, P., Havard, D., & Laneville, A. (2008a). Effect of Ice and Snow on the Dynamics of Transmission Line Conductors. In *Atmospheric Icing of Power Networks* (pp. 171–228). Springer Netherlands. https://doi.org/10.1007/978-1-4020-8531-4_5

Van Dyke, P., Havard, D., & Laneville, A. (2008b). Effect of Ice and Snow on the Dynamics of~Transmission Line Conductors. In *Atmospheric Icing of Power Networks* (pp. 171–228). Springer Netherlands. https://doi.org/10.1007/978-1-4020-8531-4_5

Van Dyke, P., & Laneville, A. (2008). Galloping of a single conductor covered with a D-section on a high-voltage overhead test line. *Journal of Wind Engineering and Industrial Aerodynamics*, *96*(6–7), 1141–1151. https://doi.org/10.1016/j.jweia.2007.06.036

Wallenius, T., & Lehtomäki, V. (2016). Overview of cold climate wind energy: challenges, solutions, and future needs. *WIREs Energy and Environment*, *5*(2), 128–135. https://doi.org/10.1002/wene.170

Wang, L., Meng, H., Wang, F., & Liu, H. (2024). Ice nucleation mechanisms and the maintenance of supercooling in water under mechanical vibration. *Results in Physics*, *59*, 107581. https://doi.org/10.1016/j.rinp.2024.107581

Waris, M. B., Ishihara, T., & Sarwar, M. W. (2008). Galloping response prediction of ice-accreted transmission lines. *The 4th International Conference on Advances in Wind and Structures*.

Wright, W. B. (1999). *User manual for the NASA Glenn ice accretion code LEWICE Version 2.0* (Issue CR-1999-209409).

Wu, T., & Snaiki, R. (2022). Applications of Machine Learning to Wind Engineering. *Frontiers in Built Environment*, *8*. https://doi.org/10.3389/fbuil.2022.811460

Wu, T., Sun, Y., Quan, X., & Yu, Z. (2024). Performance-based wind engineering for roof cladding based on vulnerability analysis of roof plate unit. *Journal of Building Engineering*, *95*, 109958. https://doi.org/10.1016/j.jobe.2024.109958

Xiu, D., & Karniadakis, G. E. (2003). Modeling uncertainty in flow simulations via generalized polynomial chaos. *Journal of Computational Physics*, *187*(1), 137–167. https://doi.org/10.1016/S0021-9991(03)00092-5

Yang, F., Zhang, H., Zhou, Q., & Liu, S. (2020). Wind-ice Joint Probability Distribution Analysis based on Copula Function. *Journal of Physics: Conference Series*, *1570*(1), 012078. https://doi.org/10.1088/1742-6596/1570/1/012078

Yu, W., Zhang, T., Lu, Y., Han, F., Zhou, Y., & Hu, D. (2020). Engineering risk analysis in cold regions: State of the art and perspectives. *Cold Regions Science and Technology*, *171*, 102963. https://doi.org/10.1016/j.coldregions.2019.102963

Yue Ming. (2018). *Icing thickness prediction model for overhead transmission lines*. New Jersey Institute of Technology.

Zerr, R. J. (1997). Freezing Rain: An Observational and Theoretical Study. *Journal of Applied Meteorology*, *36*(12), 1647–1661. https://doi.org/10.1175/1520-0450(1997)036<1647:FRAOAT>2.0.CO;2